AXIAL BEHAVIOR OF FRP CONFINED RECTANGULAR COLUMNS WITH POLYUREA

SİNAN KARAYİĞEN

MASTER'S THESIS

SUPERVISOR

Assoc.Prof.Dr. Emre AKIN

AYDIN-2021

ACCEPTANCE AND APPROVAL

The thesis entitled "AXIAL BEHAVIOR OF FRP CONFINED RECTANGULAR COLUMNS WITH POLYUREA" prepared by Sinan KARAYİĞEN, a student of the Department of Civil Engineering program at T.C. Aydın Adnan Menderes University, Graduate School of Natural and Applied Sciences, was accepted as Master's thesis by the jury below.

Date of Thesis Defence: 24/06/2021

Member : Assoc.Prof.Dr. Emre AKIN   Aydın Adnan Menderes University
(T.D.)

Member : Assoc.Prof.Dr. Ebru DURAL   Aydın Adnan Menderes University

Member : Asst.Prof.Dr. Abdullah DİLSİZ   Ankara Yıldırım Beyazıt University

APPROVAL

    This thesis was approved by the jury above in accordance with the relevant articles of the Aydin Adnan Menderes University Graduate Education and Examination Regulations and was approved on the …………………………. by from the Board of Directors of the Graduate School of Science in the …………………………. numbered decision.

Prof.Dr. Gönül AYDIN

Institute Director

ACKNOWLEDGEMENTS

First of all, I would like to thank my consultant Assoc. Prof. Dr. Emre Akın for his help and guidance. I also thank Instr. Dr. Burhan Aleessa Alam for his assistance in performing the coupon experiments. I would like to extend my endless thanks to my family, my aunt and my friends who have always supported me.

Dedicated to

My family

Sinan KARAYİĞEN

TABLE OF CONTENTS

LIST OF SYMBOLS AND ABBREVIATIONS

A_e/A_c **:** The effective confinement area ratio

A_g **:** The gross area of the specimen

ASTM C39   **:** Standard test method for compressive strength of cylindrical concrete specimens

ASTM D3039   **:** Standard test method for tensile properties of polymer matrix composite materials

b-h   **:** The column dimensions

CFRP   **:** Carbon fiber reinforced polymers

cm   **:** Centimeter

d   **:** The diameter of the specimens

D   **:** The diagonal distance of the section

ε_{cu} **:** The ultimate strain of the confined concrete

ε_{co} **:** Strain at the maximum stress of the unconfined concrete

$\varepsilon_{cu}/\varepsilon_{co}$ **:** Strain-enhancement ratio

E_{frp} **:** Modulus of elasticity of the FRP

ε_{hrup} **:** The hoop rupture strain

f_{cc} **:** The ultimate stress of the confined concrete

f_{co} **:** The maximum stress of the unconfined concrete

f_{cc}/f_{co} **:** Strength-enhancement ratio

f_{lu} **:** The confining pressure

FRP   **:** Fiber reinforced polymers

GFRP   **:** Glass fiber reinforced polymers

HPFRCC	: High-performance fiber-reinforced cement-based composite
kN	: Kilonewton
k_{s1}-k_{s2}	: The shape factors
k_1-k_2	: The confinement effectiveness coefficients
LVDT	: Linear variable displacement transducers
MPa	: Megapascal
NP	: None polyurea
P	: Polyurea
PAN	: Polyacrylonitrile
ρ_{sc}	: The cross-sectional area of the longitudinal steel
R	: Radius
t	: Thickness
UV	: Ultraviolet

LIST OF FIGURES

LIST OF PICTURES

LIST OF TABLES

ÖZET

POLYUREA ILE TAKVIYE EDILMIŞ FRP SARGILI DİKDÖRTGEN KOLONLARIN EKSENEL DAVRANIŞI

Karayigen S. Aydın Adnan Menderes Üniversitesi, Fen Bilimleri Enstitüsü, İnşaat Mühendisliği Programı, Yüksek Lisans Tezi, Aydın, 2021.

Amaç: Bu çalışma, dikdörtgen kesitli beton kolonlara lifli polimerlerle yapılan sargılamanın etkinliğinin arttırılması amacıyla FRP ceket ile dikdörtgen beton çekirdeği arasına uygulanan poliürea katmanının etkisinin irdelenmesi amacıyla yapılmıştır.

Materyal ve Yöntem: Çalışma kapsamında 23 adet 67 mm x 134 mm boyutlarında dikdörtgen kesitli beton kolon üretilmiştir. Dikdörtgen kesitli kolonların köşeleri 15 mm ve 30 mm yuvarlatılarak keskin köşelerde meydana gelebilecek gerilme yığılmalarının engellenmesi amaçlanmıştır. Üretilen dikdörtgen kesitli kolonlar tek kat ve çift kat cam lifli polimer (GFRP) ile sargılanmıştır. Dikdörtgen kesitli kolonların 10 tanesinde poliürea kaplama uygulanmıştır. Güçlendirmenin etkisini göstermek amacıyla sargılama ve köşe yuvarlatması uygulanmamış numuneler de üretilmiştir. Ayrıca test sonuçlarını mevcut bir modelle karşılaştırmak için 6 adet 150 mm çaplı eşdeğer silindir numune üretilmiştir. Tüm numuneler monotonik eksenel yüklemeye tabi tutulmuştur.

Bulgular: Beton basınç makinesi kullanılarak 23 dikdörtgen kesitli numune test edilmiştir. Test sonuçları FRP sargılanmış dikdörtgen kesitli beton numunelerde önerilen poliürea katmanının monotonik testlerde eksenel basınç dayanımı ve birim deformasyon kapasitesine etkisinin yetersiz olduğunu ortaya koymuştur. Buna rağmen önerilen poliürea katmanıyla, köşeleri 15 mm yuvarlatılmış ve çift kat GFRP sargılanmış numunelerin maksimum eksenel basınç dayanımında %1.3 artış gözlenmiştir. Bu sebepten dolayı önerilen poliürea katmanı farklı yükleme testleri altında daha başarılı sonuçlar verebilir. Ayrıca uygulanan köşe yuvarlatması ve sargılamada kullanılan FRP katman sayısı, eksenel basınç dayanımı ve birim deformasyonun

arttırılmasında başarılı olmuştur.

Sonuç: Bu çalışmayla beton çekirdek ile FRP ceket ile arasına uygulanan poliürea katmanının eksenel basınç dayanımı ve birim deformasyona etkisi incelenmiştir. Sonuçlar uygulanan poliürea katmanının FRP ile sargılanmış dikdörtgen beton kolonların eksenel davranışına olumlu etkisinin yetersiz olduğunu göstermiştir. Kullanılan laboratuvardaki ekipmanlar sebebiyle testler monotonik yükleme altında yürütülmüştür. Köşeleri 15 mm yuvarlatılmış ve çift kat GFRP ile sargılanmış numunelerde poliürea katmanının basınç dayanımını arttırması, önerilen yöntemin farklı yükleme testleri altında daha başarılı sonuçlar verme ihtimalinin olduğuna işaret etmektedir.

Anahtar Kelimeler: Beton, Güçlendirme, FRP, Poliürea, Dikdörtgen Kolon

ABSTRACT

AXIAL BEHAVIOR OF FRP CONFINED RECTANGULAR COLUMNS WITH POLYUREA

Karayigen S. Aydın Adnan Menderes University, Graduate School of Natural and Applied Sciences, Programme of Civil Engineering, Master's Thesis, Aydın, 2021

Objective: This research was carried out to investigate the effect of the polyurea layer applied between the FRP jacket and the rectangular concrete core.

Material and Methods: 23 rectangular concrete columns with cross-sectional dimensions of 67 mm x 134 mm were produced within the scope of the study. The corners of rectangular columns were rounded by 15 mm and 30 mm to prevent the stress concentrations that may occur in the sharp edges. Rectangular columns were confined with a single layer and double layer glass fiber reinforced polymer (GFRP). Polyurea coating was applied between the FRP jacket and the concrete core in 10 of the rectangular columns. Samples without confinement and corner rounding were also produced to show the effect of confinement. In addition, to compare the test results with an existing design-oriented model, six cylindrical specimens with a 150 mm diameter were produced. All specimens were subjected to the monotonic axial compressive loading.

Results: A total of 23 rectangular specimens were tested by using a compression test machine. The test results indicated that the polyurea layer that was proposed in FRP confined rectangular concrete specimens had an insufficient effect on the axial compressive strength and unit deformation capacity in the monotonic tests. The use of the proposed polyurea layer increased the maximum compressive strength of the specimens that have 15 mm rounded corners and confined by two layers of GFRP specimens (i.e. R15-2G) by 1.3%. For this reason, the recommended polyurea layer might give more successful results under different loading tests. In addition, the corner-rounding applied and the number of FRP layers used in strengthening were successful in increasing the axial compressive strength and strain capacity.

Conclusion: In this study, the effect of the polyurea layer applied between the rectangular concrete core and FRP jacket on the axial compressive strength and strain capacity was investigated. The results indicated that the positive effect of the applied polyurea layer on the axial behavior of rectangular concrete columns confined with GFRP was insufficient. Due to the setup in the laboratory, the tests were carried out under monotonic loading. The increase in the compressive strength of the specimens having 15 mm rounded corners and confined by two layers of GFRP indicates that the proposed polyurea layer might give more successful results under different loading tests.

Keywords: Concrete, Strengthening, FRP, Polyurea, Rectangular Column

1. INTRODUCTION

Turkey is located in an active earthquake zone. Earthquakes in the past have caused great loss of life and property in Turkey. To prevent this situation in the future, weak structures should be detected. After the seismic analysis of the deficient structures, the structure should be demolished or strengthened. When the inadequate structures in our country are examined, the reasons for the damages in earthquakes are summarized by Tankut (2005) as follows:

- lack of sufficient lateral rigidity
- inappropriate arrangement of reinforcement in columns
- short columns
- soft stories
- structures consisting of strong beams-weak columns
- poor concrete quality
- workmanship defects

such deficiencies result in the buildings not having the required strength, ductility and rigidity properties.

Studies on the strengthening of buildings have become very popular in recent years. The purpose of strengthening works is to increase the performance of the structure, extend its service life or increase the load-bearing capacity. The retrofitting costs may be insignificant in certain structures such as historical buildings. But in buildings such as residences, shops and schools where we live our daily lives, the cost is important. Such structures must be safe and sound. Subsequent changes in the structure, such as the elimination of walls, columns or openings cut in the floors, also damage the structural system of the building, causing problems that can lead to damage or even destruction. Such changes should not be made, if any, the necessary calculations should be made and the structure should be strengthened.

1.1. Types of Strengthening

There are two types of strengthening which are member strengthening and system rehabilitation. Some applications are made to increase the strength and/or deformation capacity of the members in the member strengthening. The flexural, shear, axial and/or torsional

behavior of the members may be issued in the member strengthening. The confinement of the columns that is applied mainly to improve the axial response is an example for this method. The column confinement is the subject of this thesis study, therefore it will be focused on this strengthening method hereafter. On the other hand, more comprehensive applications such as adding shear walls or adding new reinforced concrete frames are conducted in the system rehabilitation.

1.2. Confinement of Columns

The main aim of confinement is to improve the axial behavior of the columns which may be regarded as the most critical members for the seismic response of the structures. The axial compressive strength and deformation capacity of the columns are aimed to be increased. The column is supposed to acquire a much more ductile character after the confinement. Besides, the column confinement may also provide an improvement in terms of shear behavior.

Some techniques used for the confinement of reinforced concrete columns are:

- reinforced concrete jacketing,
- steel jacketing,
- FRP confining or jacketing.

1.2.1. Reinforced Concrete Jacketing

It is one of the most common methods used to increase the axial load capacity of columns. Initially, the number and dimensions of the steel reinforcement required within the jacket are determined. This method have the potential to considerably increase the axial load-carrying capacity and ductility of the columns. However, the molds and preparation of the molds are relatively expensive. The sheathing material (i.e. concrete) is brittle and therefore the improvement in the ductility is less than the increase in the axial load-carrying capacity. When this method is applied, the cross-sectional area and size of the column increase. This situation may cause undesirable stiffness increases in the structure. As a result, seismic demands on the building may also increase. In this method, the cross-sectional area and resulting mass of the column increase which may also alter the seismic demands (Raza et al., 2019).

To avoid the increased stiffness and mass caused by the increase in the cross-sectional area, studies have been carried out on high-performance materials that do not increase the cross-sectional area and mass. Cho et al. (2012) used high-performance fiber-reinforced cement-based composite (HPFRCC) mortar in the plastic hinge area of the column to reduce bending and shear cracks in the plastic hinge area and also saw a significant reduction in undesirable stiffness.

1.2.2. Steel Jacketing

In this method, the confining reinforcement is provided outside the element by means of steel sections placed at each corner that are in full contact with the concrete. These steel sections are then connected by welded lateral steel plates at a certain spacing all along the column height. In this way, both the axial load capacity of the column is increased and higher ductility is achieved. The steel jacket does not contribute to the bending capacity of the column since the continuity between the floors cannot be achieved (Tankut 2005). Also, steel jacketing is proved to effectively enhance the shear strength of the columns. Although the increase in the mass due to this method is lower compared to the reinforced concrete jacketing, it still increases the dead loads and the cross-sectional dimensions of the structure (Raza et al., 2019).

1.2.3. Confinement by Fiber Reinforced Polymers

The fiber-reinforced polymers are formed by combining certain polymers with fibers having high tensile strength. In the last three decades, FRP's have been used as an important rehabilitation material in the building industry. FRP's provide higher mechanical properties compared to traditional building materials. They may be used in different forms such as FRP plates, FRP rebars, FRP sheets (fabrics). Both its superior mechanical properties and ability to be produced in desired sizes and easy to process have enabled FRP materials to be used in many areas. Some properties of FRP's can be listed as:

- corrosion resistance,
- high tensile strength,
- high stiffness,
- lighter weight compared to conventional steel,

- ease of application.

In addition, the use of FRP especially for the rehabilitation purposes do not restrict the use of the building compared to traditional methods and does not add additional dead weight to the building.

As an alternative to the reinforced concrete and steel jacketing, the concrete columns of existing structures can be externally confined by high-strength FRP composites. The FRP materials may be tailored with desired length and width, and required thickness may be arranged by the number of confining layers. Furthermore, the fibers may be placed in various directions to meet the specific structural requirements.

FRP's consist of two basic components which are polymer matrix and fibers. The favorable properties of these two components are gathered to constitute a new material for a specific purpose as it is the case for all composite materials. These components of FRP's are introduced briefly in the following paragraph.

The matrices are strong adhesives (i.e. epoxy). They also protect fibers from the environmental influences. The matrices support the fibers, holding the composite material together. The loads on the composite material are first met by the matrix and transferred to the fibers by the matrices. Matrix materials can be composed of polymer, metal or ceramic material. There are many types of fibers such as carbon, glass, aramid and basalt. Some of the most used fiber types are reviewed below.

The carbon fibers differ according to their production methods such that there are polyacrylonitrile (PAN) and pitch-based carbon fibers. PAN-based ones are used in the repair and strengthening works in the construction sector due to their high strength properties. PAN-based carbon fibers differ among themselves as ultra-high modulus, high modulus and high strength. All of them are produced in the same way, but their curing temperatures are different. They are much thinner than steel despite having a much higher tensile strength than steel (Sonnenschein et al., 2016). Carbon fibers do not absorb water and are resistant to all kinds of alkalis and solvents. Pitch-based carbon fibers offer higher modulus compared to PAN-based carbon fibers (Avci et al., 2019).

Due to their versatile use and low cost, glass fibers are the most used fiber type (Sonnenschein et al., 2016). E-glass is the most commonly used fiber type in FRP composite

applications in the reinforced concrete structures. E-glass consists of alumo-calcium borosilicates and does not contain alkali. It has high electrical resistance. S-glass has a magnesium aluminosilicate composition with very high tensile strength and is resistant to high temperatures. AR-glass, i.e. alkali-resistant glass, is highly resistant to high alkaline environments such as concrete.

Aramid is from the polyamide class. There are two types as meta-aramid and para-aramid (kevlar). Kevlar is more widely used. Aramid is the fiber with the highest tensile strength/density ratio among the reinforcement fibers used in the market. It has the lowest density among the most used fibers. Compared to glass, it has 40% lower density than glass. It is not resistant to moisture and UV rays (Sonnenschein et al., 2016).

There are different types of process methods for the application of FRP's. The wet lay-up process is the most popular one used in the FRP strengthening. When used for the column confinement, the wet-lay-up process includes the wrapping of epoxy-impregnated unidirectional fiber sheets around the column, such that the fibers are oriented in the lateral direction. But the concrete surface should be cleaned of dust and roughnesses should be removed before wrapping. The primer material is applied to remove the dust and the putty material is applied to remove the roughness on the surface which provide a better adhesion. Epoxy should also be applied to the concrete surface with a roller. Then the column is wrapped with epoxy-impregnated fabrics.

1.3. Purpose of the Study

The FRP materials has been proven to be most effective materials when used for the confinement of columns with circular sections (Lam and Teng, 2003a; Ozbakkaoglu and Akin, 2012). Yet, the efficient use of this material for the confinement of circular sections is reported to be limited due to the premature failure. This premature failure takes place by rupturing of the confining jacket at a strain level lower than the strain capacity of FRP either given by the manufacturer or obtained in the tensile coupon tests. Different explanations are provided for the possible reasons of the early rupture (Lam and Teng, 2003a). One of them is related with the local stress concentrations caused by the non-uniform deformations of concrete in the lateral direction when subjected to axial loading.

Akın et al. (2020) utilized polyurea as a padding material between the concrete and confining jacket. The concrete section used in the study was circular. The main aim was to

protect the FRP jacket from the stress concentrations caused by the deforming concrete and thus to obtain a more uniform lateral stress distribution on the jacket. The researchers stated that although the rupture strain improved considerably, this did not lead to a significant improvement in the axial strength and strain capacity under monotonic loading. However, the additional polyurea layer enhanced not only the rupture strain but also the axial strength and strain capacity under cyclic loading.

On the other hand, the studies on the square and rectangular columns revealed that further stress concentrations at the sharp edges (i.e. corners) also reduce the effectiveness of the FRP jacket (Lam and Teng, 2003b). This lead a lower confinement efficiency in the case of columns with square/rectangular sections compared to circular sections. Consequently, the rounding of corners by grinding is suggested to reduce the stress concentrations at the sharp edges. A minimum corner radius is required for rounding the sharp edges to obtain a sufficient confinement which is still defined to be less efficient compared to that of an equivalent circular section. And the effectively confined area remains to be lower than the gross-sectional area.

In this thesis study, the improvement in the confinement efficiency, provided by means of using an additional polyurea layer between the concrete and FRP jacket, as suggested by Akın et al. (2020) was taken as a basis. It was aimed to reduce the stress concentrations not only caused by the deforming concrete but also those produced at the corner regions of the rectangular sections. The polyurea layer was supposed to provide a more uniform confinement effect within the section and increase the effectively confined sectional area. As a consequence, a higher rupture strain, ultimate axial strength and aixal strain capacity was expected.

1.4. Thesis Organization

This thesis consists of seven chapters. The first chapter, the introduction, is presented above. In Chapter 2, the studies in the literature on the strengthening of reinforced concrete columns are summarized. In Chapter 3, the materials and methods used in the experimental study are explained. The test results are presented in Chapter 4. In Chapter 5, the discussions about the results are presented. In Chapter 6, a theoretical investigation is presented to compare the test results with predictions of an existing design-oriented model. Finally, in Chapter 7, the results of the study are summarized.

2. LITERATURE REVIEW

2.1. General Introduction

In this section, some of the previous studies related to the confinement of concrete columns are presented.

2.2. Strengthening Reinforced Concrete Columns with Concrete Jacketing or Steel Jacketing

Strengthening of reinforced concrete columns with concrete or steel jacketing are the traditional and frequently used strengthening methods. Vandoros and Dritsos (2008) experimentally examined the effectiveness of the reinforcement of the columns with a concrete jacket. Three different concrete jacketing methods were used in the study; welding jacket stirrup ends to each other, inserting dowels and jacket stirrup end welding, and placing bent down steel connector bars welded to the original column longitudinal reinforcement bars. Samples were subjected to cyclic loading. In addition, two CFRP confined specimens were presented in the study for comparison. The concrete jackets increased ductility, strength, and durability. However, the strength degradation was less after reaching the maximum load in the specimens strengthened with CFRP. Strengthening with CFRP increased ductility significantly more compared to the concrete jacketing. The reinforced concrete column jackets with welded stirrup ends have increased the strength and ductility of the columns. The welding of the stirrup ends prevented the longitudinal reinforcement from buckling. This resulted in a higher maximum load capacity.

Pudjisuryadi et al. (2015) experimentally studied the performance of square reinforced concrete columns confined by steel angle collars. Two specimens were used as control specimens and confined with conventional stirrups. The other three specimens were externally confined only by steel angle collars. The volumetric ratios of steel collars of these three specimens were changing. A total of 5 specimens were prepared and subjected to combined axial and lateral loads. The behavior of specimens with traditional stirrups was compared with specimens confined with external steel angle collars. The steel angle collar specimens were found to be very ductile and failed at higher drifts than specimens confined with stirrups. The specimen with the lowest volumetric ratio of steel collars showed brittle (non-ductile) behavior,

and specimens with higher volumetric ratios of collars showed ductile behavior. As the volumetric ratio of the steel collars increased, the behavior of the specimens improved.

2.3. Strengthening Reinforced Concrete Columns with Fiber Reinforced Polymers

The strengthening of the columns with FRP has been very popular in recent years. Many studies have been done on this subject and studies are still ongoing. The effects of many parameters such as the number of FRP layers, types of FRP, unconfined concrete strength, corner radius, the orientation of the fibers, shape and size effect, and slenderness were investigated.

Stepanek et al. (2016) experimentally investigated the load-bearing capacity of concrete columns reinforced with FRP fabric and the factors affecting this. The number of layers, the direction of the fabric, the size, and the effect of slenderness were examined. The columns in two different lengths, termed as short and long, were produced. While the height-diameter ratio is 2 for short columns, this value is 14.5 for long columns. Thus, they aimed to observe the effect of shape and slenderness. As a result of the study, even if multi-layer unidirectional FRP was applied to high columns, the expected increase in the load-carrying capacity could not be achieved. Slenderness has been shown to significantly reduce the effect of confinement as a result of the low lateral pressure. It has been observed that the confinement efficiency in long columns is low due to the slenderness effect. The activation of the fibers and the fragility of the elements affect the final behavior of the FRP confined columns.

Mirmiran et al. (1998) examined some parameters that may affect the efficiency of FRP wrapping in the columns. The main parameters were the section shape, height of the columns, and the bond between column and FRP jacket. Two different cross-sectional shapes, square and circular, were examined. To examine the effect of slenderness, samples with 4 different heights were tested. Three different winding methods were used: single-wrapped multi-layer bonded sample, single-wrapped and multi-layer unbonded sample, and mechanical bonding by connector ribs. As a result of the study, it was seen that the confinement efficiency was higher in the circular sections than square sections. It was concluded that the effect of length:diameter ratios in the range of 2:1 and 5:1 did not affect the strength and ductility of the section. It has been found that the confinement efficiency increases with the mechanical bond.

Raval and Dave (2013) experimentally studied the behavior of three different shapes of GFRP confined columns. A total of fifteen columns (five circular, five square and five rectangular) were cast. The diameter of the circular sections were 170 mm. The cross-sectional dimensions of the square and rectangular samples were 150 mm x 150 mm and 110 mm x 210 mm, respectively. All columns were one meter in height. Three columns from each group were unconfined and used as control specimens, while the other two columns were confined with one layer of GFRP. All specimens were tested under axial compression. The results showed that the axial load carrying capacity increased from rectangular to square and from square to circular in constrained columns. Circular columns wrapped by GFRP exhibited more ductile behavior compared to square and circular columns wrapped with GFRP. GFRP wrapped rectangular columns had higher deformation compared to square and circular columns. The best confinement efficiency was achieved in circular columns.

Safan (2004) examined the behavior of short reinforced concrete columns wrapped with GFRP. Forty-five specimens were cast. These specimens were divided into control, one layer GFRP wrapping, two layers of GFRP wrapping, two layers of GFRP wrapping with surface roughening, and partial wrapping test groups. All specimens were subjected to concentric compressive loads. Test parameters were number of GFRP layers, wrapping method and column surface roughness degree. The results showed that FRP wrapping improved strength and ductility in square columns. The stress concentrations at the corners caused the jacket to rupture at an early stage. It was concluded that higher ultimate load values can be achieved by rounding the corners. The column surface roughening did not affect the behavior.

Benzaid et al. (2008) investigated the behavior of square columns confined with GFRP. Square reinforced concrete specimens with dimensions of 100 mm x 100 mm and a height of 300 mm were used in the study. These specimens were divided into 3 groups as without corner rounding, 8 mm corner radius, and 16 mm radius. The main test parameters were the number of layers and the corner radius. As a result of the experiments, they concluded that FRP confinement increases the axial load carrying capacity and ductility of the columns. And these increments are directly proportional to the number of layers. Also, the confinement zone was increased by using a larger corner radius, and thus the stress concentrations that may occur at sharp corners were reduced.

Different types of wrapping affect the efficiency of the confinement. Pham et al. (2016) experimentally investigated the effects of different arrangements of FRP on the mechanics of confinement. In the experimental study, glass FRP and carbon FRP fabrics were wrapped

around the samples in three different arrangements as fully, partially, and non-uniformly. Twenty-one FRP wrapped concrete cylinder specimens and three non-strengthened reference specimens were subjected to monotonic loading. The concrete cylinder specimens have a diameter of 150 mm and a height of 300 mm. The results showed that the partial and non-uniformly wrapped samples in the group of heavily confined samples provided higher axial strain value than the fully wrapped samples. The actual rupture strain of the FRP jackets varied with the winding arrangement. The strain efficiency factor had the highest value in the non-uniform winding and the smallest value in the partial winding.

Rousakis and Tepfers (2001) investigated the mechanical behavior of carbon FRP confined concrete. The low and high strength concrete specimens were obtained by using three different concrete mixing ratios for 27 specimens in total. 6 plain specimens were examined under monotonic axial compression. Teflon sheets were used between concreteand steel plates to obtain less friction and to examine the effect of teflon deformation on axial displacement in one specimen from each group. The remaining 21 specimens were subjected to axial monotonic and cyclic loads. To examine the overlap length effect, 3 specimens were wrapped with a lap length of 50 mm, 100 mm, and 150 mm. A fixed overlap length of 150 mm was used in the remaining samples. The overlap length used in the FRP jackets directly affects the behavior of concrete. The early rupture occurred in case of insufficient overlap. This situation was observed in the specimen with a lap length of 50 mm. The effect of using teflon on axial displacement was negligible. The lateral strain measured during the rupture of the confined concrete at the FRP surface was found to be less than half of the rupture strain capacity of the carbon fibers. Also, the strength-enhancement increased in direct proportion to the number of layers.

Kalyoncuoglu et al. (2013) experimentally studied the confinement of columns which are subjected to corrosion with FRP sheets. Four reinforced concrete columns were prepared by using extremely low-strength concrete and plain reinforcing bars. Except for the reference specimen, three samples were subjected to a corrosion process for comparison. The first of these three specimens were not repaired/confined, the second was repaired with structural repair mortar, and the third was repaired using mortar and confined by CFRP sheets. The results showed that the structural repair mortar increased the strength of the reinforced concrete columns. On the other hand, CFRP confinement significantly improved the ductility as well as the strength of the column.

Lam and Teng (2009) experimentally investigated the behavior of concrete wrapped with FRP under cyclic compression. Eighteen specimens with the same dimensions were tested in

two groups. Three samples in each group were unstrengthened control samples. The six samples remaining in the groups were wrapped with one or two layers of CFRP. For three FRP-wrapped specimens in each series, cyclic compression was applied, including unloading and reloading cycles, at several unloading displacement values before failure. An overlap length of 150 mm was applied to the wrapped samples. All samples wrapped with FRP failed due to a rupture of the FRP jacket. The envelope curve of the stress-strain response of concrete wrapped with FRP was little affected by the unloading/reloading cycles. Unloading/reloading cycles slightly improved the FRP hoop rupture strain values. The repeated unloading/reloading cycles affected permanent strain and stress deformations.

Green et al. (2006) investigated columns wrapped with FRP materials under extreme conditions such as -40 degrees or fire. In addition, corroded columns were also examined. As a result of the study, it was observed that freezing-thawing and exposure to low temperature cause sudden deterioration in the FRP-wrapped columns. FRP windings reduce the corrosion rate in corroded columns and if they are made with proper insulation, FRP-wrapped columns had flame resistance for up to 4 hours.

2.4. Effect of Using Polyurea on Strengthening

In the FRP confined concrete, the roughnesses and deteriorations on the concrete surface, or the stress concentrations that may occur due to the deformed concrete may cause the material used in wrapping to rupture before reaching its ultimate strain capacity. Therefore, Akın et al. (2020) experimentally investigated the effect of polyurea coating applied between concrete and FRP on strengthening. In the study, 28 concrete cylinder specimens with low strength were tested under axial pressure. The cylinder specimens had a diameter of 150 mm and height of 300 mm. Eighteen specimens were subjected to monotonic axial loading and the remaining ten specimens were subjected to cyclic axial loading. Test parameters were loading type, presence of polyurea, and the number of FRP layers. The polyurea coating increased the rupture strains of the CFRP sheet. It was seen that the use of polyurea increased the confinement effectiveness, but the effect of this increase was more clear in the cyclic loading than the monotonic loading. It was stated that the presence of polyurea could increase the number of loading cycles. Comparing the polyurea coated and uncoated CFRP wrapped specimens, it was seen that the

ultimate strain capacity of the polyurea coated specimens was approximately 20% higher. On the other hand, the ultimate compressive strength of the polyurea-coated specimens was found to be slightly lower. The presence of polyurea slightly reduced the plastic strains in the specimens.

Parniani and Toutanji (2015) experimentally studied the behavior of concrete beams coated with polyurea. The behavior of five reinforced concrete beams was investigated. A beam was tested without the polyurea coating and used as a control specimen. Two different levels of polyurea thickness of 2.5 mm and 5 mm were used in the study. The beams were subjected to four-point monotonic and fatigue loading. Test parameters were coating thickness and number of cycles. Polyurea coating improved flexural and shear capacity of the structural members. Under fatigue loading, the polyurea coating showed close behavior at two thickness levels. The use of polyurea increased the flexural capacity of beams by 9.2% and 17.4% for the 2.5 mm and 5 mm thickness levels, respectively. The polyurea coating improved ductility, but when the coating thickness was twice, the ductility was not improved as expected.

2.5. Strengthening Concrete Columns with Other Materials

Different materials and methods have been used in the rehabilitation of structural elements, and new strengthening methods have been investigated. Choi et al. (2012) experimentally studied the effect of using different types of shape memory alloy wire on the strengthening of the columns. The shape memory alloy wires used were nickel-titanium-niobium and nickel-titanium. Six circular columns with a diameter of 400 mm and a height of 1400 mm were prepared and subjected to the axial compressive test. Five specimens had 50% lap splice of the longitudinal reinforcements thus, half of the bars were spliced from the starter bars projecting from the foundation. The remaining specimen was used as a reference specimen without lap splice. SMA wires were attached to the concrete with anchors. The results showed that nickel-titanium-niobium alloy wires are more suitable for the use in structural strengthening compared to nickel-titanium alloys, as they can be used in a wider temperature range. The shape memory alloy wire jackets achieved ductile behavior without a decrease of strength in the lap spliced specimens.

3. MATERIAL AND METHODS

3.1. General Introduction

The effect of polyurea on the FRP confinement of low-strength concrete with rectangular sections was experimentally evaluated in this thesis study. The experimental program was carried out in Aydın Adnan Menderes University Civil Engineering Department Laboratory. All processes including concrete casting, wrapping of the specimens, and tests were carried out in the laboratory. The following sections provide the experimental program in details.

3.2. Test Specimens

23 rectangular specimens were prepared. The dimensions of the specimens were 67 x 134 mm. In addition to the rectangular sections, six specimens with equivalent circular cross-sections (ie equivalent cylindrical specimens) were prepared. The cylindrical specimens had a diameter of 150 mm which was chosen to be equal to the diagonal length of the rectangular sections. The height of all samples was 300 mm. The low-strength concrete with a compressive strength of 15 MPa was used in the preparation of the specimens. The details of the test specimens were illustrated in Figure 3.1.
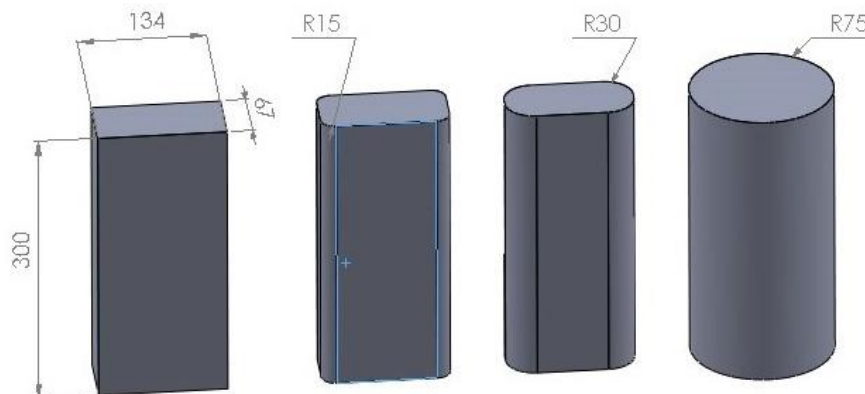

Figure 3.1. The details of specimens (3D forms)

3.3. Test Configuration

The concrete specimens were divided into 12 groups. Two or three identical specimens were prepared for each group. The first group RRef contains unconfined rectangular specimens. The second group RRef-2G-NP designates a specimen with sharp edges having two layers of GFRP where no polyurea was applied. The third group R15-1G-NP consists of specimens with a 15 mm corner radius, wrapped with one layer of GFRP and without polyurea. The fourth group R15-1G-P consists of specimens with a 15 mm corner radius, wrapped with one layer of GFRP and with polyurea. The fifth group R15-2G-NP consists of specimens with a 15 mm corner radius, wrapped with two layers of GFRP and without polyurea. The sixth group R15-2G-P consists of specimens with a 15 mm corner radius, wrapped with two layers of GFRP and with polyurea. The seventh group R30-1G-NP consists of specimens with a 30 mm corner radius, wrapped with one layer of GFRP and without polyurea. The eighth group R30-1G-P consists of specimens with a 30 mm corner radius, wrapped with one layer of GFRP and with polyurea. The ninth group R30-2G-NP consists of specimens with a 30 mm corner radius, wrapped with two layers of GFRP and without polyurea. The tenth group R30-2G-P consists of specimens with a 30 mm corner radius, wrapped with two layers of GFRP and with polyurea. The eleventh group EC-1G-NP includes the equivalent cylindrical specimens that wrapped with one layer of GFRP and without polyurea. The last group EC-2G-NP includes the equivalent cylindrical specimens that wrapped with two layers of GFRP and without polyurea.

In summary, in the naming of the specimens, the first letters R or EC designates the cross-sectional shape of the specimen for rectangular and equivalent circular, respectively. In the rectangular specimens, the numbers after the R designates corner radius as 15 mm or 30 mm. Only, in the reference specimen without any rounding of the corners "Ref" stands instead of corner radius. After that, the number of GFRP layers used in the confinement given as 1G or 2G which means one or two layers of GFRP, respectively. Then, the presence of polyurea is mentioned with or without polyurea coating as P and NP, respectively.

The EC-1G-NP and EC-2G-NP groups were included in the study because the test results of these groups will be used in the analytical study. The results of these cylindrical specimens were used in the model predictions according to Lam and Teng (2003b).

Table 3.1. The test matrix

TEST GROUP	CORNER RADIUS (mm)	NUMBER OF FRP LAYERS	NUMBER OF SPECIMENS
RRef	-	-	2
RRef-2G-NP	-	2	1
R15-1G-NP	15	1	3
R15-1G-P	15	1	3
R15-2G-NP	15	2	3
R15-2G-P	15	2	3
R30-1G-NP	30	1	2
R30-1G-P	30	1	2
R30-2G-NP	30	2	2
R30-2G-P	30	2	2
EC-1G-NP	-	1	3
EC-2G-NP	-	2	3

3.4. Preparation of the Formwork

The formwork was prepared for the experimental study. The wooden plates were used to prepare the formwork. The thicknesses of the wooden plates were 20 mm. The plates were cut into the required parts with a jigsaw, and then all parts were clamped together with screws (Picture 3.1). Existing cylindrical molds (150 mm in diameter) available in the laboratory were used for casting equivalent circular specimens.

Picture 3.1. The formwork

3.5. Preparation of the Specimens

In this section, the concrete mixing ratios and pouring of the samples used in the experimental study are explained.

3.5.1. Concrete Mix Proportions

Table 3.2 shows the concrete mix proportions used to obtain a low-strength concrete. The ordinary cement was used. The water/cement ratio was approximately 0.7. The maximum size of the aggregates used was less than 15 mm.

Table 3.2. The concrete mix design proportions

Material	Sand	Aggregate (maximum size=15 mm)	Cement	Water	Total
Weight Proportions (%)	19	58	12	11	100

3.5.2. Casting of the Concrete and Curing Process

The formwork was cleaned and oil was applied to the inner surfaces of the formwork to facilitate the removal process (Picture 3.2). For the specimens with corner radius, the brackets obtained from the 3D printer were used. The brackets used to round the corners of the rectangular specimens is shown in Picture 3.3. The concrete that had been prepared according to the mixing ratios was poured into molds (Picture 3.4). During casting, each segment was compacted by using tamping rods. This was done to prevent honeycomb formations within the concrete.

Picture 3.2. The formwork after oil applied into inner surfaces

Picture 3.3. The brackets

Picture 3.4. The formwork after casting the concrete

The formwork was removed after a week and the curing process started. The water was sprayed onto the samples for this purpose and no curing pool was used. The concrete specimens were cured for 7 days. After the curing process, the surfaces of the concrete specimens were cleaned off dust. The ends of the specimens were covered with high-strength mortar to distribute the load evenly in the subsequent axial compression tests (Picture 3.5). The mechanical properties of the high-strength mortar are given in Table 3.3.

Table 3.3 The mechanical properties of the high-strength mortar

Compressive strength (MPa)	Modulus of elasticity (GPa)	Bonding strength to concrete (MPa)
>60 (28 days)	>20 (28 days)	>2 (28 days)

Picture 3.5. The specimens after capping the ends

3.6. Strengthening of the Specimens with Polyurea and GFRP

In case of the specimens without polyurea coating, the two-component primer (Picture 3.6.a) was applied to the surfaces of the specimens to remove the dust. The primer was prepared by mixing two components according to the proportions provided by the manufacturer. After this application, the specimens without polyurea coating were ready for the confinement by GFRP (Picture 3.6.b).

Picture 3.6. (a) The components of the primer **(b)** The specimens after application of primer

In case of the specimens with polyurea coating, the polyurea layer was utilized as a secondary material under the GFRP jacket (i.e. between the core concrete and GFRP layer). Polyurea has properties such as high adhesion to concrete surfaces, moisture resistance, superior elongation at break, high flexibility and tear resistance. Polyurea has been used in civil engineering to protect steel reinforcement from corrosion and to provide flexural strengthening for the reinforced concrete beams (Akın et al., 2020). In this study the polyurea was supposed to protect the GFRP material from the stress concentrations not only caused by the expanding concrete under axial compression but also those produced at the corner regions of the rectangular sections. The single-component polyurea primer (Picture 3.7.a) was applied to the concrete surface by using a roller first (Picture 3.7.b). After the application of the polyurea primer, the specimens were ready for the polyurea application. The cold polyurea that was used in the study has two components (Picture 3.7.c) which does not require heating and enables cold application. Some mechanical properties of the polyurea were presented in Table 3.4. The components of polyurea were mixed properly according to the instructions of the manufacturer. After waiting three hours after the primer as the manufacturer suggested, the polyurea was applied to the surface of the specimens by using a roller (Picture 3.7.d).

Finally, after waiting three hours, the second layer of polyurea was applied to the specimens. Approximately 2 mm polyurea layer thickness was obtained at the end of the application.

Table 3.4. The mechanical properties of the polyurea

Elongation at break	≥ 600%
Tensile strength	≥ 9 MPa
Adhesion to concrete	≥ 2 MPa

Picture 3.7. (a) The polyurea primer, **(b)** the polyurea primer application, **(c)** the components of the polyurea and **(d)** polyurea application

The specimens in the RRef group were left without confinement to have the axial response of the unconfined concrete. The other specimens were confined by one or two layers of GFRP according to the test matrix.

The unidirectional GFRP with a thickness of 0.2 mm was used as the confinement material. The wet-lay-up technique was applied for the confinement of specimens. Before

starting the wrapping process, GFRP sheets were prepared by cutting them in the determined dimensions where an overlapping length of 150 mm was also taken into account (Picture 3.8). The two components of the epoxy were mixed properly according to their weight proportions (Picture 3.9). After that, the epoxy was applied to the lateral surfaces of the specimens with a roller. The GFRP sheets which had been cut in the pre-determined dimensions were impregnated with epoxy. The epoxy impregnated GFRP sheets were carefully wrapped around the concrete specimens to provide all fibers in the lateral direction, preventing any wavy alignment. The wrapping was continued after the first layer and had a 150 mm overlap at the end of the confinement. In the specimens with two layers of confinement, the overlapping of the second layer of confinement was provided in the same location with the overlapping of the first layer. The mechanical properties of the epoxy used in the confining process is supplied by manufacturer and given in Table 3.5. Picture 3.10 shows the specimens after the strengthening process.

Table 3.5. The mechanical properties of the epoxy

Compressive strength	≥ 80 MPa
Tensile strength	≥ 30 MPa
Adhesion to concrete	≥ 4 MPa
Mixing ratios by weight	Unit A : 2 and Unit B: 1

Picture 3.8. GFRP sheets prepared with the determined dimensions

Picture 3.9. The components of the epoxy
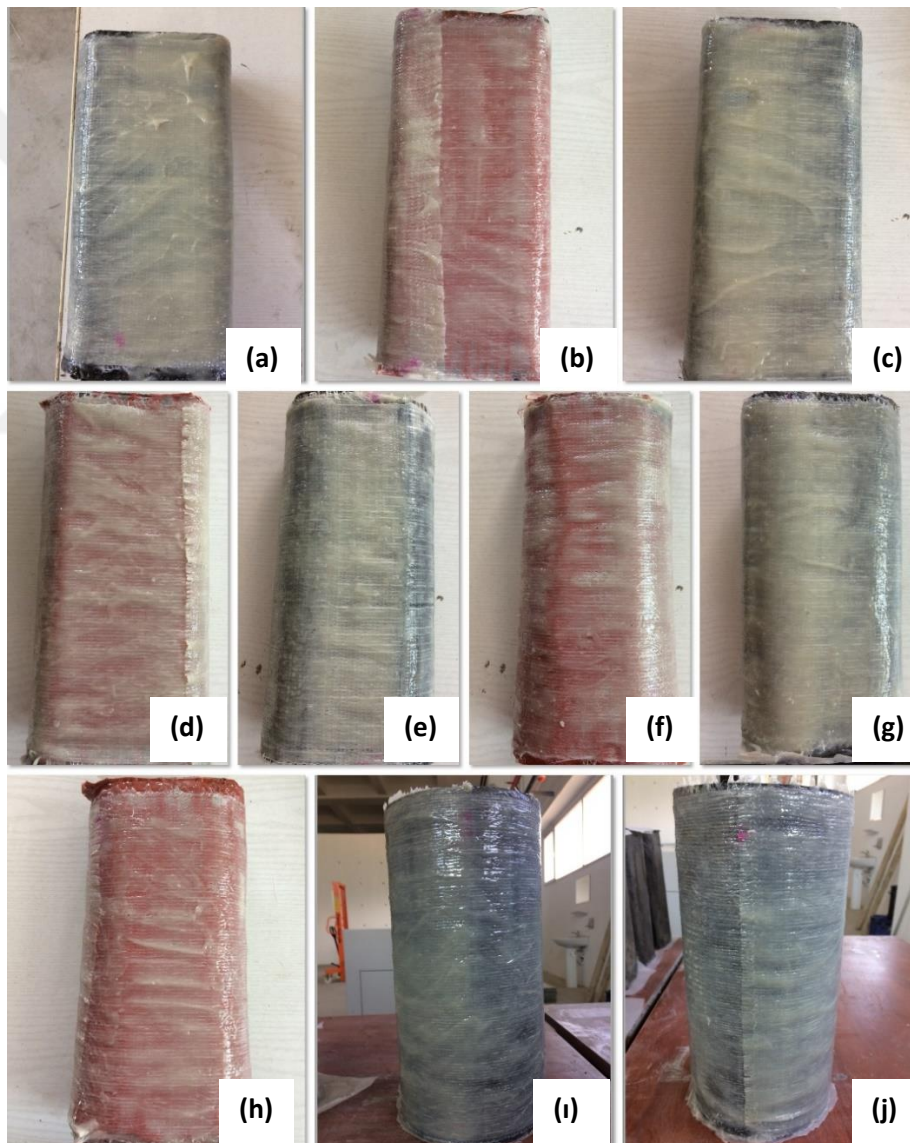
Picture 3.10. The specimens after strengthening process completed, **a)** R15-1G-NP, **b)** R15-1G-P, **c)** R15-2G-NP, **d)** R15-2G-P, **e)** R30-1G-NP, **f)** R30-1G-P, **g)** R30-2G-NP, **h)** R30-2G-P, **ı)** EC-1G-NP, **j)** EC-2G-NP

3.7. Mechanical Properties of GFRP

The mechanical properties of GFRP were found by tensile coupon tests according to ASTM D3039 (2017). Six coupon samples with a single GFRP layer were prepared, however the results of the four samples could be used due to premature failure of two samples. The width and length of the coupons were 15 mm and 250 mm, respectively. GFRP thickness was 0.2 mm. The coupon samples were placed between two steel tabs with a length of 50 mm at each end. The steel tabs and GFRP were bonded with epoxy. These steel tabs were placed between the grips of the tensile testing machine. The coupon test results are presented in Table 3.6 in terms of tensile strength, rupture strain capacity and modulus of elasticity.

Table 3.6. Mechanical Properties of GFRP

Coupon	Tensile Strength, MPa	Average Tensile Strength, MPa	Rupture Strain, %	Average Rupture Strain, %	Modulus of Elasticity, MPa	Average Modulus of Elasticity, MPa
Coupon 1	934.4		1.97		50000	
Coupon 2	1020.8	982.625	2.23	1.995	54000	50250
Coupon 3	1244.4		2.12		51500	
Coupon 4	730.9		1.66		45500	

3.8. Test Setup

The compression tests were carried out using a 3000 kN capacity testing machine. However, a separate load cell with 600 kN axial load capacity was placed under the specimens, which determines the ultimate load capacity of the test setup (Figure 3.2). All specimens were subjected to the axial monotonic compressive loading. The axial deformations were measured by linear variable displacement transducers (LVDT's). The two LVDT's were placed 180º apart from each other. To measure the lateral deformations and rupture strain of the confining jacket, three strain gauges with a gauge length of 10 mm (two along the long side and one along the short side) were placed at the mid-height of all GFRP-wrapped rectangular specimens (Figure 3.3). Again, three strain gauges were placed on the circular specimens. Two separate data acquisition system were used to collect the measured data, one was for the data from the load cell and LVDT's and the other one was for the data from the strain gauges.
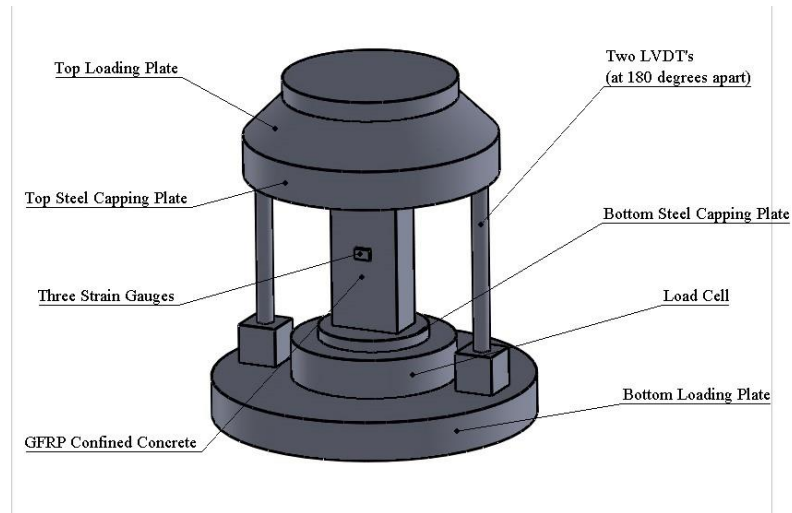
Figure 3.2. Test setup drawing (3D form)
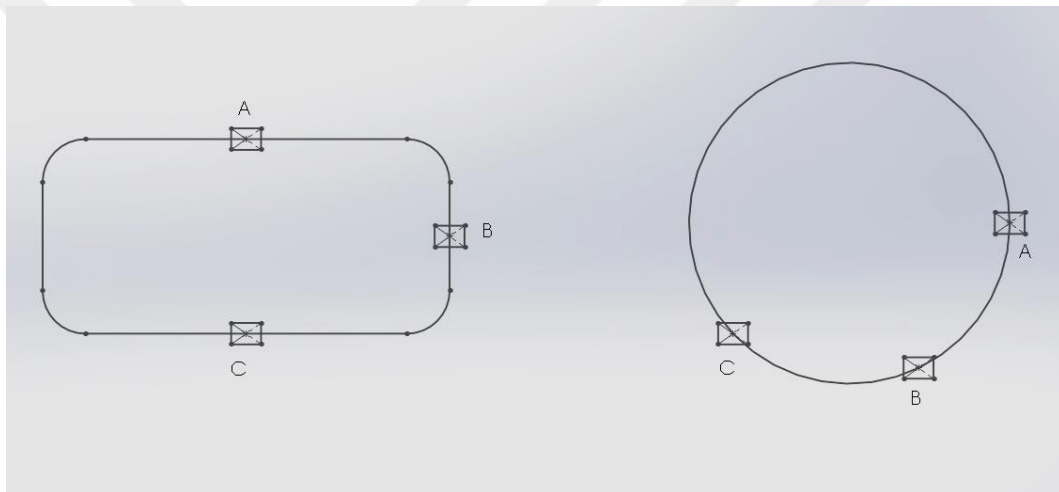
Figure 3.3. Locations of the strain gauges of the confined rectangular and circular specimens

3.9. Test Process

The specimens were carefully placed into the testing machine (Picture 3.11). Then the strain gauges were connected to the data acquisition system that was used for strain data. The LVDT's and load cell were connected to the related data acquisition system. Tests were carried out according to ASTM C39 (2020) by using constant stress (0.25 MPa/s) increments at each loading step. All results were recorded using the data acquisition systems. The tests were terminated after the rupture of the GFRP confined specimens. The tests of unconfined concrete specimens were terminated after 15-20 percent loss of ultimate axial strength. The photos showing the failure of the specimens were taken after the tests.

Picture 3.11. Test setup

4. RESULTS

4.1. General Introduction

Results obtained from experiments are given in this section. The failure modes of the specimens, axial stress-strain curves, the hoop strain curves and ultimate conditions (i.e. ultimate axial strength and strain capacity) are presented. These results are evaluated in the discussion section.

4.2. Failure Modes

The specimens RRef-1 and RRef-2 suddenly failed after reaching their axial load capacity (i.e. unconfined concrete compressive strength). The failure was brittle. These unconfined specimens after the test are shown in Picture 4.1. During the test of the specimen with sharp edges and two layers of GFRP (Rref-2G-NP), the failure was observed close to the corner of the mid-height. This may be due to the stress concentrations in the specimens with sharp edges (Picture 4.2).

The specimens in the R15-1G-NP group failed mostly around the mid-height as shown in Picture 4.3. In the R15-1G-P group, two specimens failed at mid-height and the other one failed at the corner close to the bottom of the specimen (Picture 4.4). The rupture zone of the R15-1G-NP specimens were larger than the same specimens with polyurea coating.

Two of the specimens in the R15-2G-NP group failed along the long side of the section around the mid-height and the other one failed in top portion along the long side as shown in Picture 4.5. In the R15-2G-P group, all specimens failed near the mid-height corners (Picture 4.6). In the R30-1G-NP group, specimens failed at the mid-height along the long side (Picture 4.7). For the specimens in the R30-1G-P group, one specimen failed at the rounded corner and the other one failed at mid-height near to the corner as shown in Picture 4.8. The specimens in the R30-2G-NP group both failed near the corner; however one of them was in bottom portion and the other one was in top portion (Picture 4.9). On the other hand, when the polyurea coating was used, the failure zone was shifted to the mid-height along the long side in the R30-2G-P group (Picture 4.10).

In the test group of EC-1G-NP and EC-2G-NP, two specimens of each group failed by rupturing of GFRP at the top portion and the remaining specimen in each group failed at the bottom portion of the specimen (Picture 4.11 and Picture 4.12).

The failure was not explosive in the specimens confined with GFRP having 15mm and 30 mm corner radius and popping noises were heard before the rupture. However, the rupture in the circular concrete specimens was more explosive and occurred suddenly. The existence of polyurea layer seems not to cause any apparent difference in the type of failure.

Picture 4.1. Failure modes of unconfined specimens

Picture 4.2. The failure mode of the specimen with sharp edges confined with two layers of GFRP

Picture 4.3. Failure modes of R15-1G-NP specimens

Picture 4.4. Failure modes of R15-1G-P specimens

Picture 4.5. Failure modes of R15-2G-NP specimens

Picture 4.6. Failure modes of R15-2G-P specimens

Picture 4.7. Failure modes of R30-1G-NP specimens

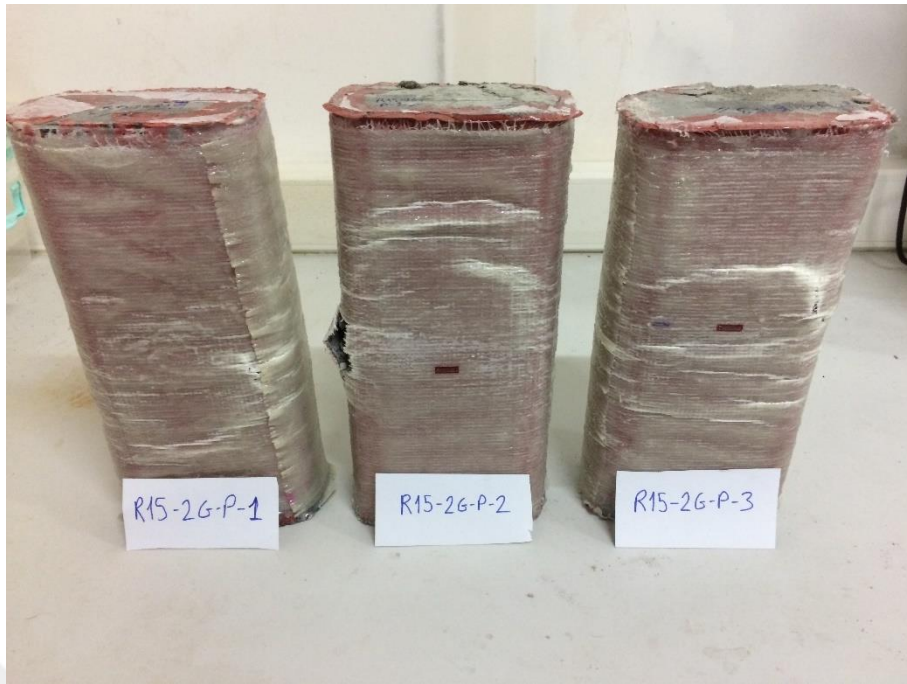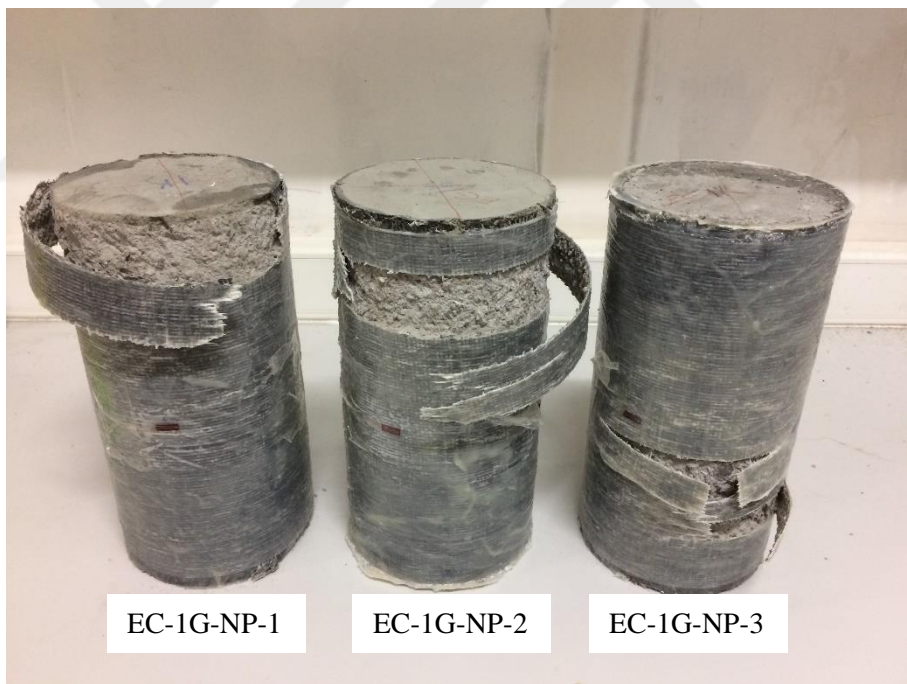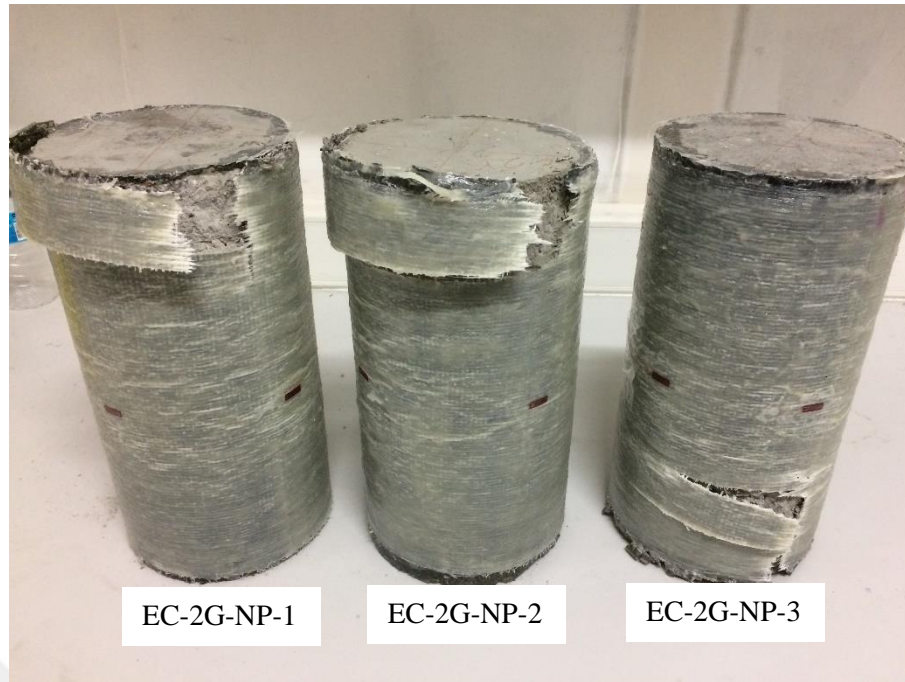**Picture 4.8.** Failure modes of R30-1G-P specimens

Picture 4.9. Failure modes of R30-2G-NP specimens

Picture 4.10. Failure modes of R30-2G-P specimens

Picture 4.11. Failure modes of EC-1G-NP specimens

Picture 4.12. Failure modes of EC-2G-NP specimens

4.3. Test Results

The axial stress is found by dividing the load capacity by the cross-sectional area. The axial strain is found by dividing the average of the displacements measured by the two LVDTs by the specimen height. The ultimate axial compressive strength (f_{cc}) and axial strain capacity (ε_{cu}) were obtained in each test. Besides, the strength-enhancement (f_{cc}/f_{co}) and strain-enhancement ratios ($\varepsilon_{cu}/\varepsilon_{co}$) were calculated. It should be noted that f_{co} and ε_{co} are the average ultimate compressive strength and corresponding strain from the tests of unconfined specimens. .

In the previous chapters, it was mentioned that the FRP jacket used for the confinement generally ruptures before reaching its ultimate strain capacity, either that was supplied by the manufacturer or determined by the tensile coupon tests. Therefore a strain efficiency factor is defined as the ratio of the rupture strain of the FRP jacket ($\varepsilon_{h,rup}$) to the tensile strain capacity of the FRP material (ε_{frp}) as shown in Eqn 1. The strain efficiency factor is calculated for each test specimen considering the coupon test results for the tensile strain capacity of the material (Table 3.6).

$$k_{\varepsilon} = \frac{\varepsilon_{h,rup}}{\varepsilon_{frp}} \qquad (1)$$

These test results are provided in Table 4.1. According to this table, the highest axial strength was obtained in the R30-2G-NP group as an average of 26.22 MPa. Among the confined specimens, the lowest axial strength was observed in the R15-1G-P group as an average of 14.80 MPa. The specimens in the R30-2G-P group had the highest axial strain as an average of 0.0397. Among the confined specimens, the lowest axial strain was observed in the RRef-2G-NP test specimen with a value of 0.0147. The results given in Table 4.1 will be assessed in the following chapter in a more detailed manner.

4.4. Stress-Strain Curves

The axial compressive stress vs. strain diagrams were plotted for all the specimens. These stress-strain diagrams are presented in Figures 4.1-12 seperately for each test group.

The unconfined specimens showed brittle behavior with a sudden decrease in strength after reaching the ultimate as expected (Figure 4.1). For almost all confined specimens, except RRef-2G-NP, the first ascending portion of the stress-strain curves was followed by an ascending second portion with a lower slope that started after the maximum stress value of the unconfined concrete (Figures 4.2-12). Although axial strength and deformability could be enhanced slightly in the specimen RRef-2G-NP compared to the unconfined specimens, the similar strength reduction after the ultimate level took place, which demonstrates an insufficient confinement (Figure 4.2). Besides, the second slope was almost zero for almost all specimens having one-layer of GFRP in the case of 15 mm corner radius which indicates a threshold confinement for the concrete strength and geometry used in the specimens (Figures 4.3-4). The use of two layers of GFRP confinement increased the slope of the second portion considerably, leading to enhanced axial strength and strain capacities for the specimens with 15 mm corner radius (Figures 4.5-6). In all specimens with 30 mm corner radius, the confinement may be regarded as sufficient with considerable enhancement in the axial strength and strain capacity (Figures 4.7-10).

Table 4.1. The test results

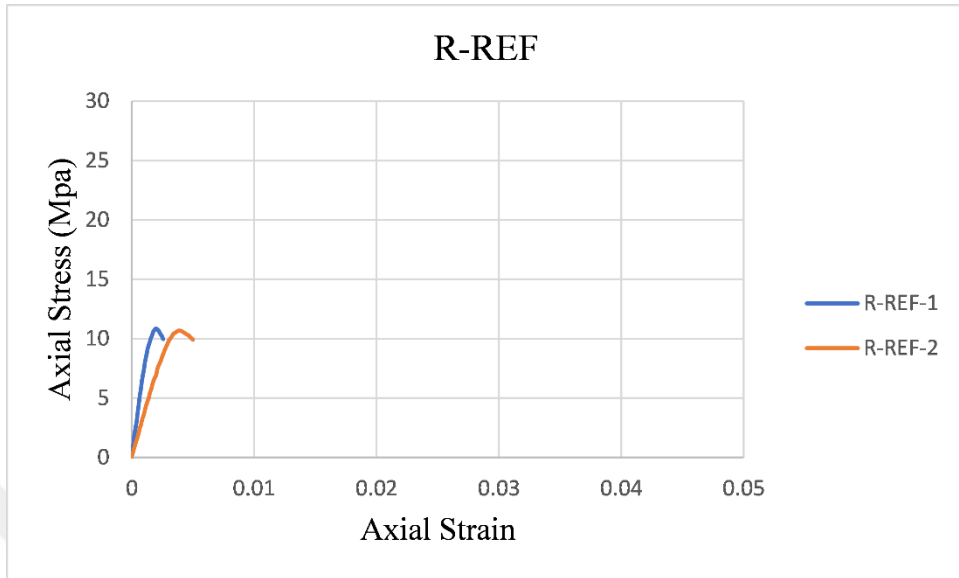| GROUP	Specimen	f_{cc} or f_{co}, MPa	Average f_{cc} MPa	ε_{cu}	Average ε_{cu}	f_{cc}/f_{co}	Average f_{cc}/f_{co}	$\varepsilon_{cu}/\varepsilon_{co}$	Average $\varepsilon_{cu}/\varepsilon_{co}$	ε_{hrup}	Average ε_{hrup}	k_e $\varepsilon_{hrup}/\varepsilon_{coupon}$	Average k_e
RRef (Unconfined)	1	10.85	10.76	0.0019	0.0028	1	1	1	1	–	–	–	–
	2	10.67		0.0038									
RRef-2G-NP	1	15.26	15.26	0.0147	0.0147	1.41	1.41	5.25	5.25	0.0053	0.0053	0.26	0.26
R15-1G-NP	1	16.78	15.40	0.0209	0.0216	1.55	1.43	7.46	7.72	0.0107	0.0120	0.53	0.59
	2	13.97		0.0206		1.29		7.35		0.0112		0.56	
	3	15.47		0.0234		1.43		8.35		0.0139		0.69	
R15-1G-P	1	14.02	14.80	0.0161	0.0164	1.30	1.37	5.75	5.85	0.0068	0.0081	0.34	0.40
	2	16.80		0.0155		1.56		5.53		0.0080		0.40	
	3	13.58		0.0176		1.26		6.28		0.0094		0.47	
R15-2G-NP	1	20.93	22.67	0.0278	0.0315	1.94	2.10	9.92	11.26	0.0122	0.0131	0.61	0.65
	2	24.74		0.0377		2.29		13.46		0.0131		0.65	
	3	22.36		0.0291		2.07		10.39		0.0138		0.69	
R15-2G-P	1	23.84	22.98	0.0327	0.0328	2.21	2.13	11.67	11.72	0.0076	0.0114	0.38	0.57
	2	21.92		0.0338		2.03		12.07		0.0139		0.69	
	3	23.18		0.0320		2.15		11.42		0.0126		0.63	
R30-1G-NP	1	15.46	15.54	0.0241	0.0268	1.43	1.44	8.60	9.58	0.0106	0.0102	0.53	0.50
	2	15.63		0.0296		1.45		10.57		0.0097		0.48	
R30-1G-P	1	14.37	14.85	0.0250	0.0238	1.33	1.38	8.92	8.51	0.0079	0.0089	0.39	0.44
	2	15.34		0.0227		1.42		8.10		0.0099		0.49	
R30-2G-NP	1	25.55	26.22	0.0372	0.0384	2.37	2.43	13.28	13.71	0.0114	0.0124	0.57	0.61
	2	26.89		0.0396		2.49		14.14		0.0133		0.66	
R30-2G-P	1	21.68	22.75	0.0437	0.0397	2.01	2.11	15.60	14.19	0.0076	0.0091	0.38	0.45
	2	23.83		0.0358		2.21		12.78		0.0105		0.52	
EC-1G-NP	1	15.29	15.49	0.0290	0.0280	1.42	1.44	10.35	10	0.0163	0.0172	0.81	0.86
	2	14.84		0.0283		1.37		10.10		0.0157		0.78	
	3	16.36		0.0267		1.52		9.53		0.0195		0.97	
EC-2G-NP	1	24.59	22.80	0.0405	0.0381	2.28	2.11	14.46	13.6	0.0133	0.0146	0.66	0.72
	2	20.24		0.0358		1.88		12.78		0.0138		0.69	
	3	23.58		0.0382		2.19		13.64		0.0164		0.82	

Figure 4.1. Stress-strain curve of the unconfined specimens (RRef group)
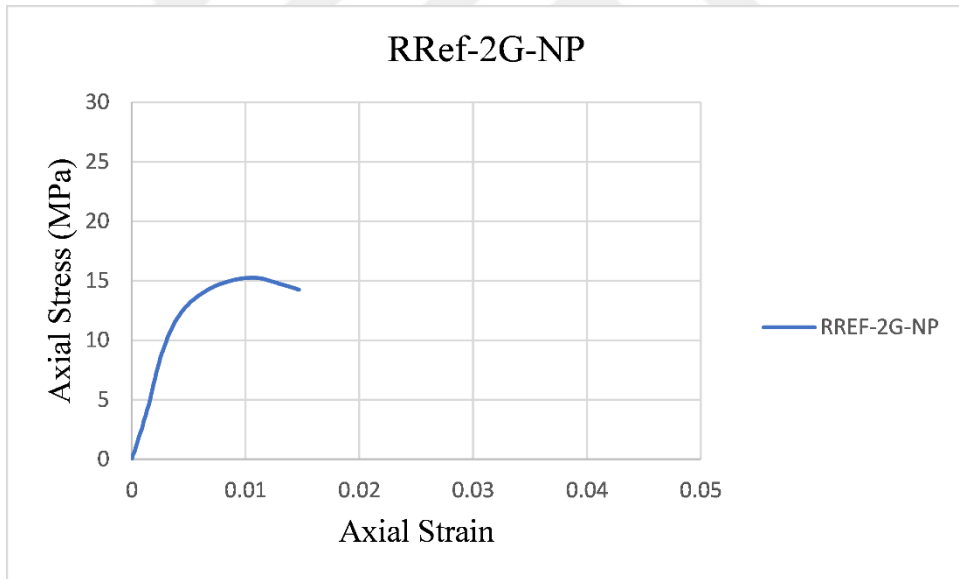

Figure 4.2. Stress-strain curve of the specimen with sharp edges confined with two layers GFRP (RRef-2G-NP group)
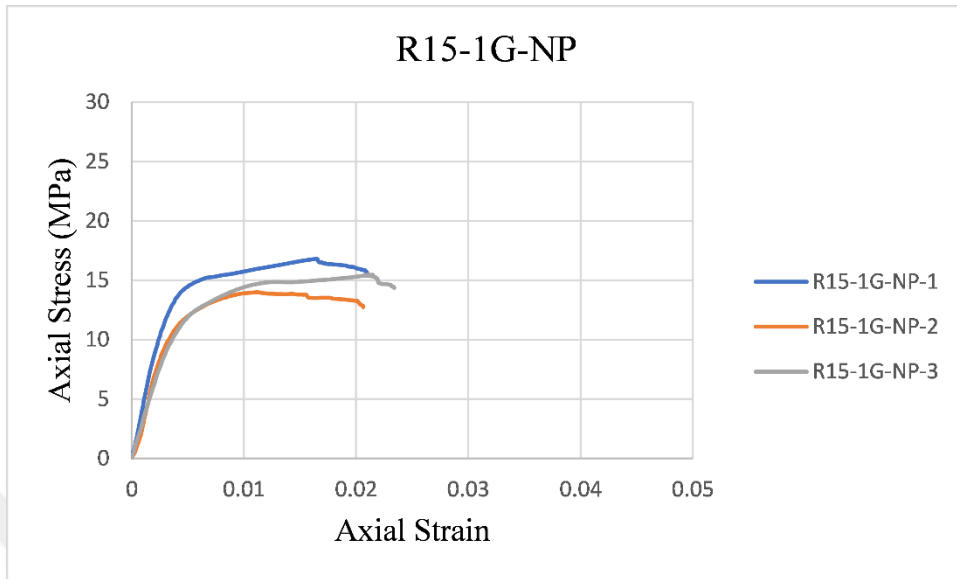
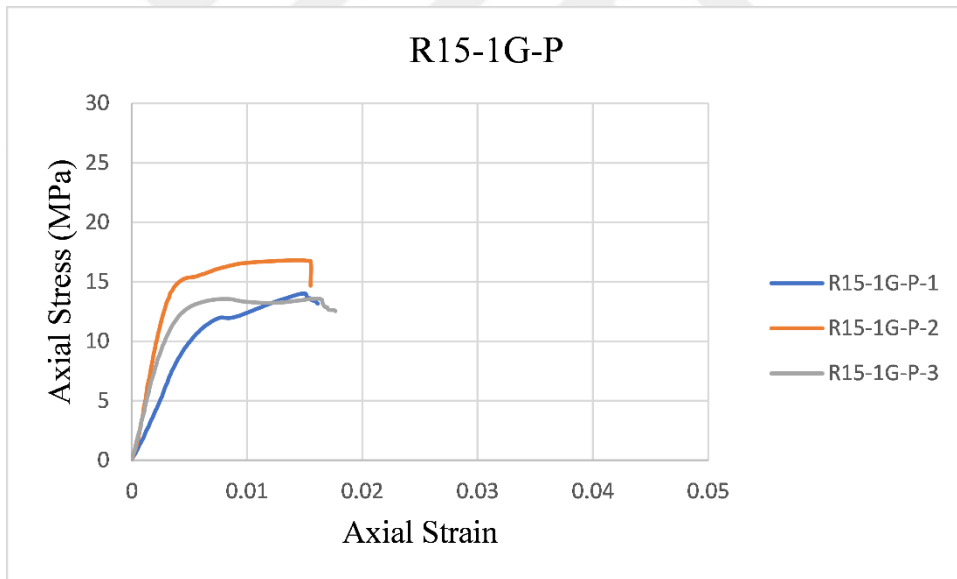**Figure 4.3.** Stress-strain curve of the specimens in the R15-1G-NP group

Figure 4.4. Stress-strain curve of the specimens in the R15-1G-P group
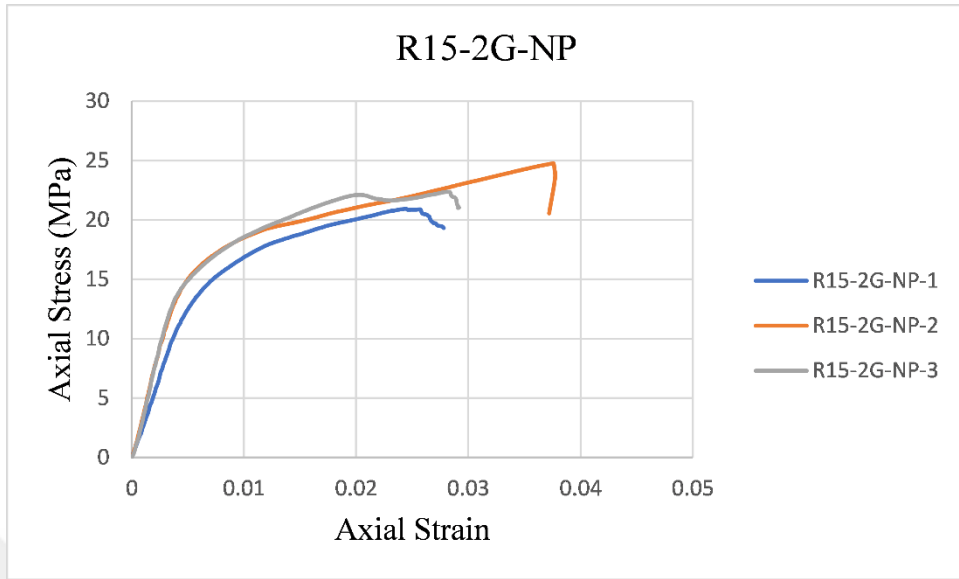
Figure 4.5. Stress-strain curve of the specimens in the R15-2G-NP group
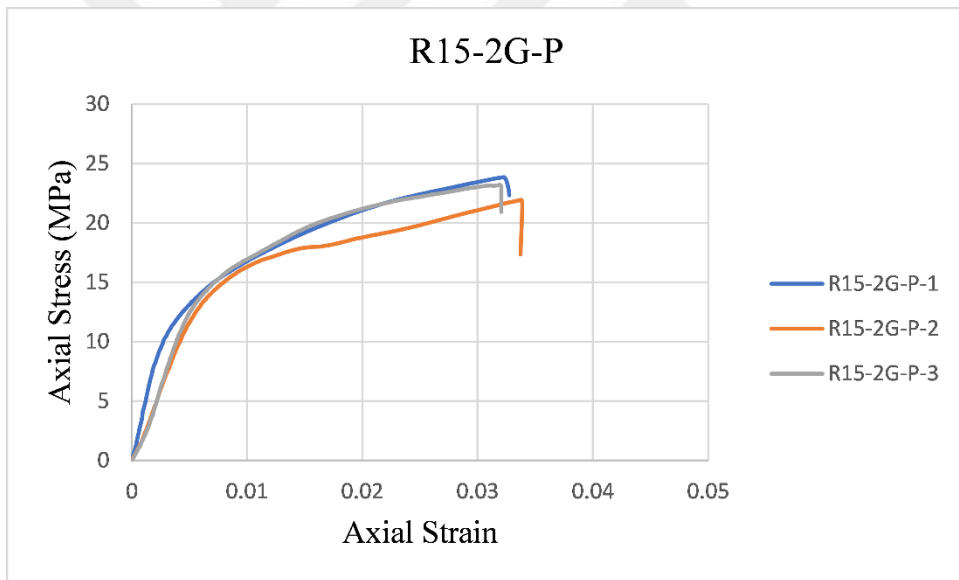

Figure 4.6. Stress-strain curve of the specimens in the R15-2G-P group

Figure 4.7. Stress-strain curve of the specimens in the R30-1G-NP group
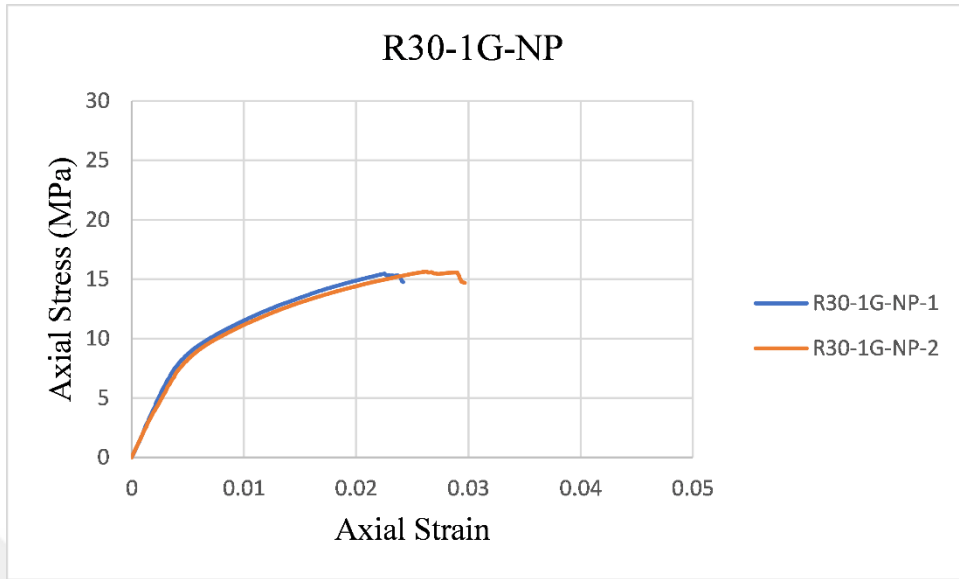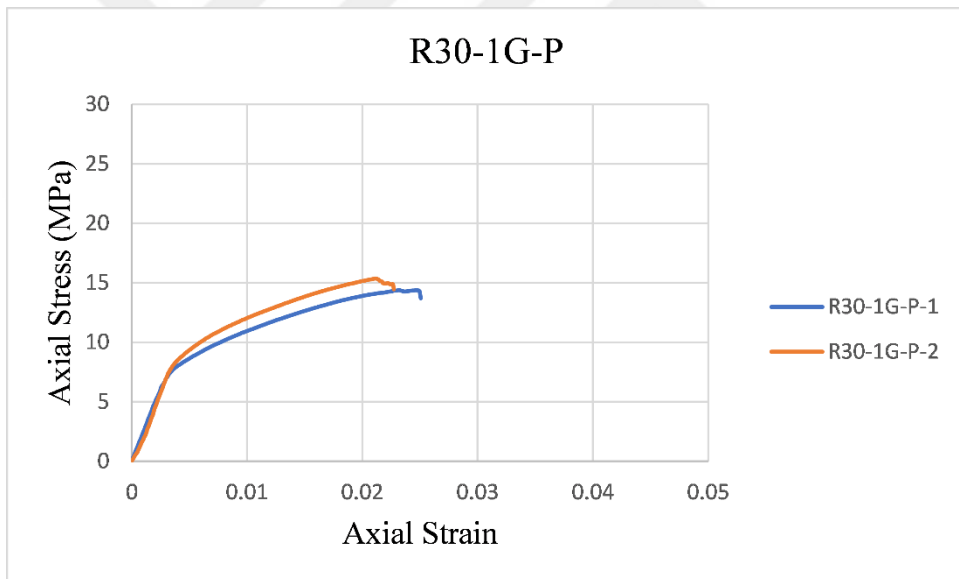

Figure 4.8. Stress-strain curve of the specimens in the R30-1G-P group
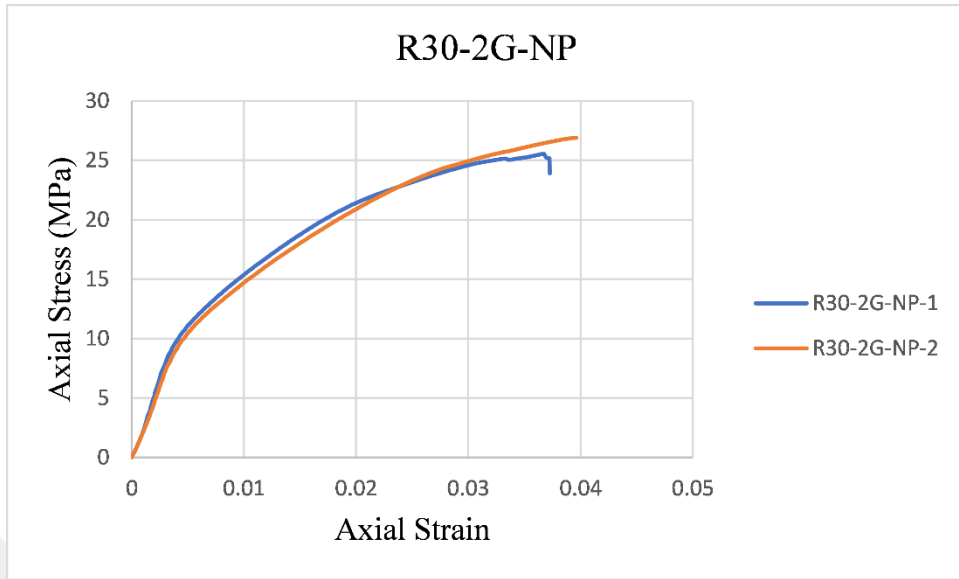
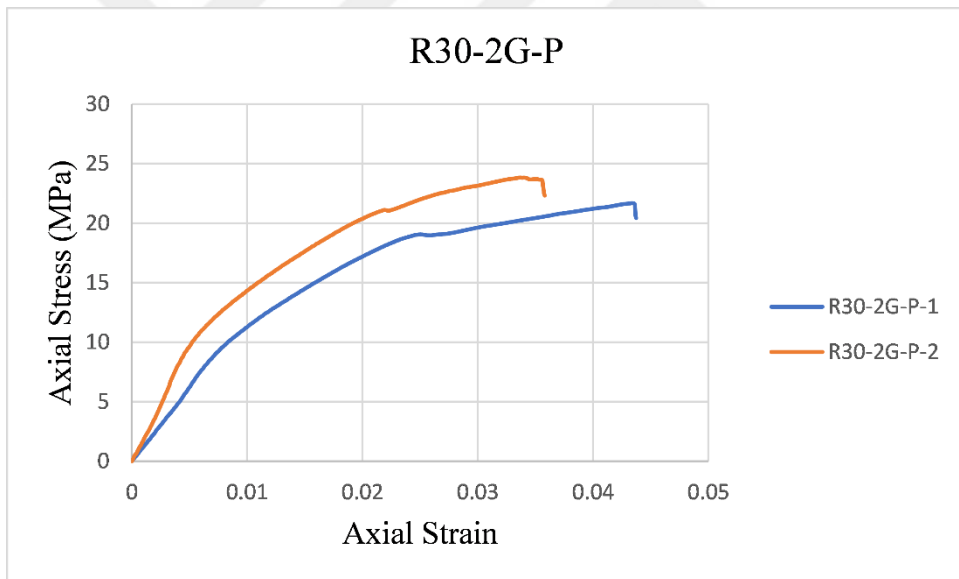**Figure 4.9.** Stress-strain curve of the specimens in the R30-2G-NP group

Figure 4.10. Stress-strain curve of the specimens in the R30-2G-P group
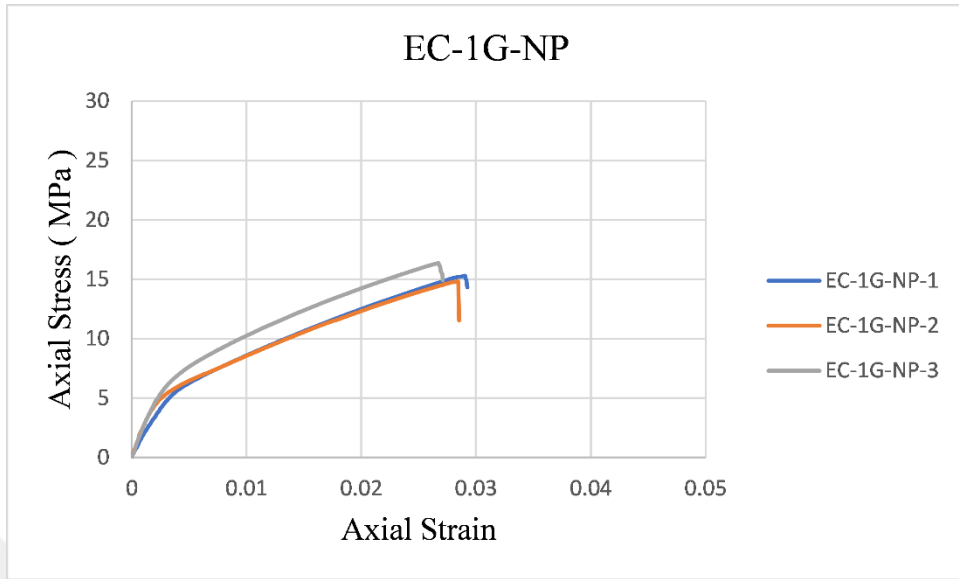
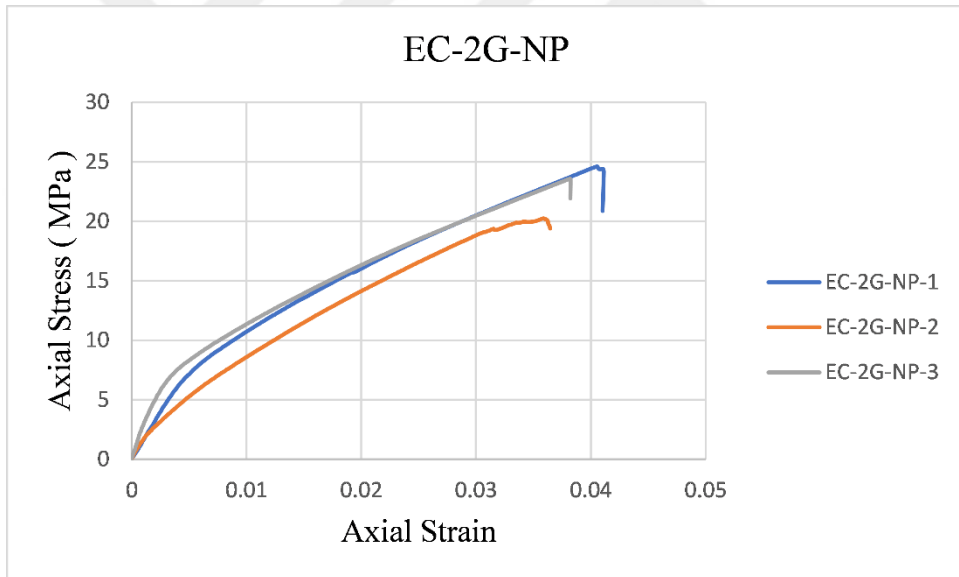**Figure 4.11.** Stress-strain curve of the specimens in the EC-1G-NP group

Figure 4.12. Stress-strain curve of the specimens in the EC-2G-NP group

Figure 4.13. Comparison of the sharp-edged specimen (RRef-2G-NP) with the specimens that have a 15 mm corner radius

In Figure 4.13, the axial stress-strain graphs are given for all specimens with a 15 mm corner radius in comparison to that of reference specimen, RRef-2G-NP. The axial behaviors of the specimens having 15 mm corner radius that were confined with one layer of GFRP were similar to the RRef-2G-NP specimen or slightly enhanced. By considering that the sharp-edged reference specimen (RRef-2G-NP) has two layers of GFRP confinement, it may be stated that rounding of the corners even with a radius of 15 mm enhanced axial response considerably.

In Figure 4.14, the RRef-2G-NP specimen was compared with the specimens that have a 30 mm corner radius. The positive effect of rounding the corners with a larger 30 mm radius in terms of enhanced axial response is more obvious in Figure 4.14.

In order to understand the effect of number of GFRP layers, the specimens with the same corner radius and same property in terms of polyurea were compared among themselves (Figure 4.15). The increase in the confinement thickness increased the effectiveness of the confinement in terms of both strength and ductility significantly. However, this seems to be more considerable in the test groups with 15 mm corner radius.
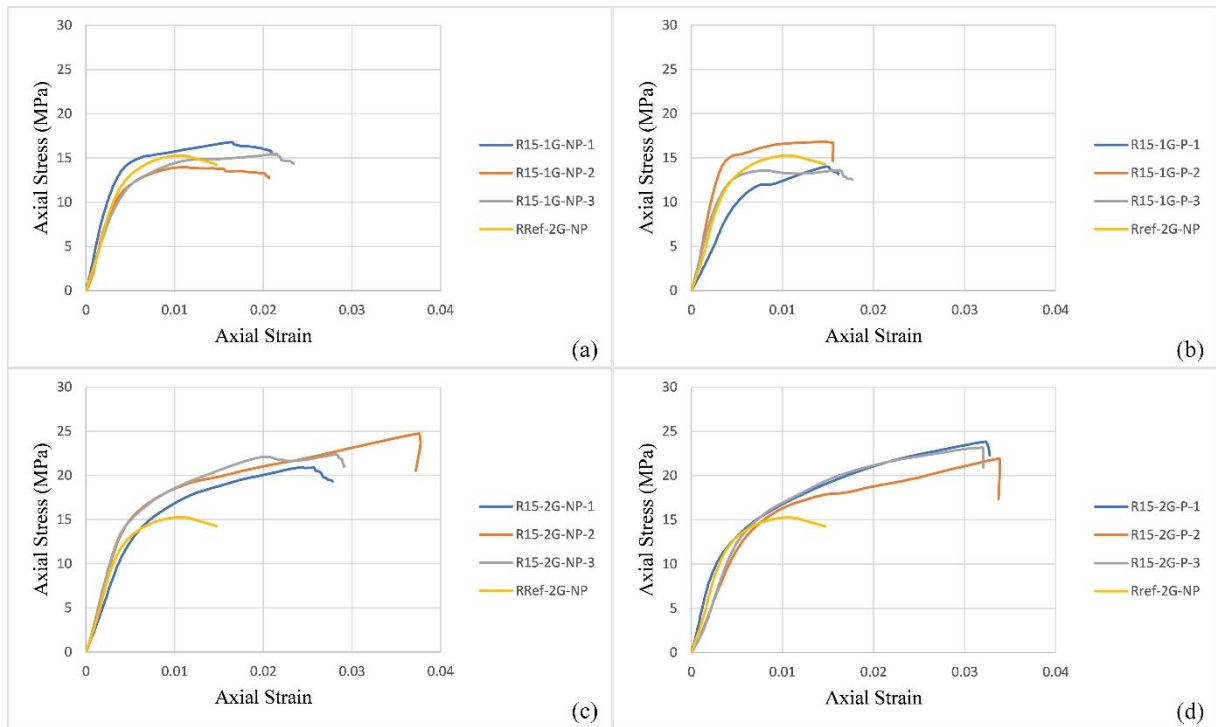
43
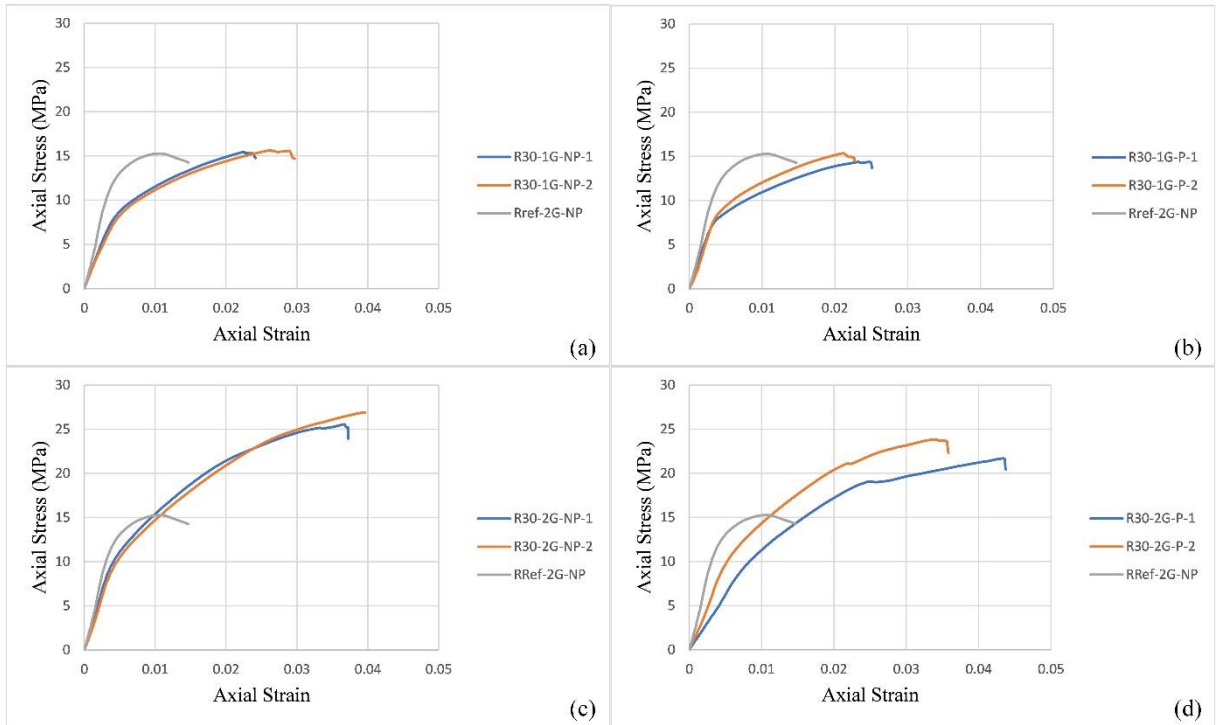
Figure 4.14. Comparison of the sharp-edged specimen (RRef-2G-NP) with the specimens that have a 30 mm corner radius

In Figure 4.16, the specimens confined with the same number of GFRP layers and the same corner radius were compared to observe the effect of polyurea. The positive effect of polyurea layer to the confinement efficiency could not be observed in the rectangular low-strength concrete columns under axial monotonic compression tests.

The specimens with same number of GFRP layer and same property in terms of polyurea were compared to observe the effect of rounding the corners (Figure 4.17). Although Figure 4.13-14 shows this effect, the direct comparison of companion specimens with either 15 or 30 mm corner radius may be beneficial to assess the effect of corner radius more clearly. Further discussions according to these figures will be conducted in the next chapter.
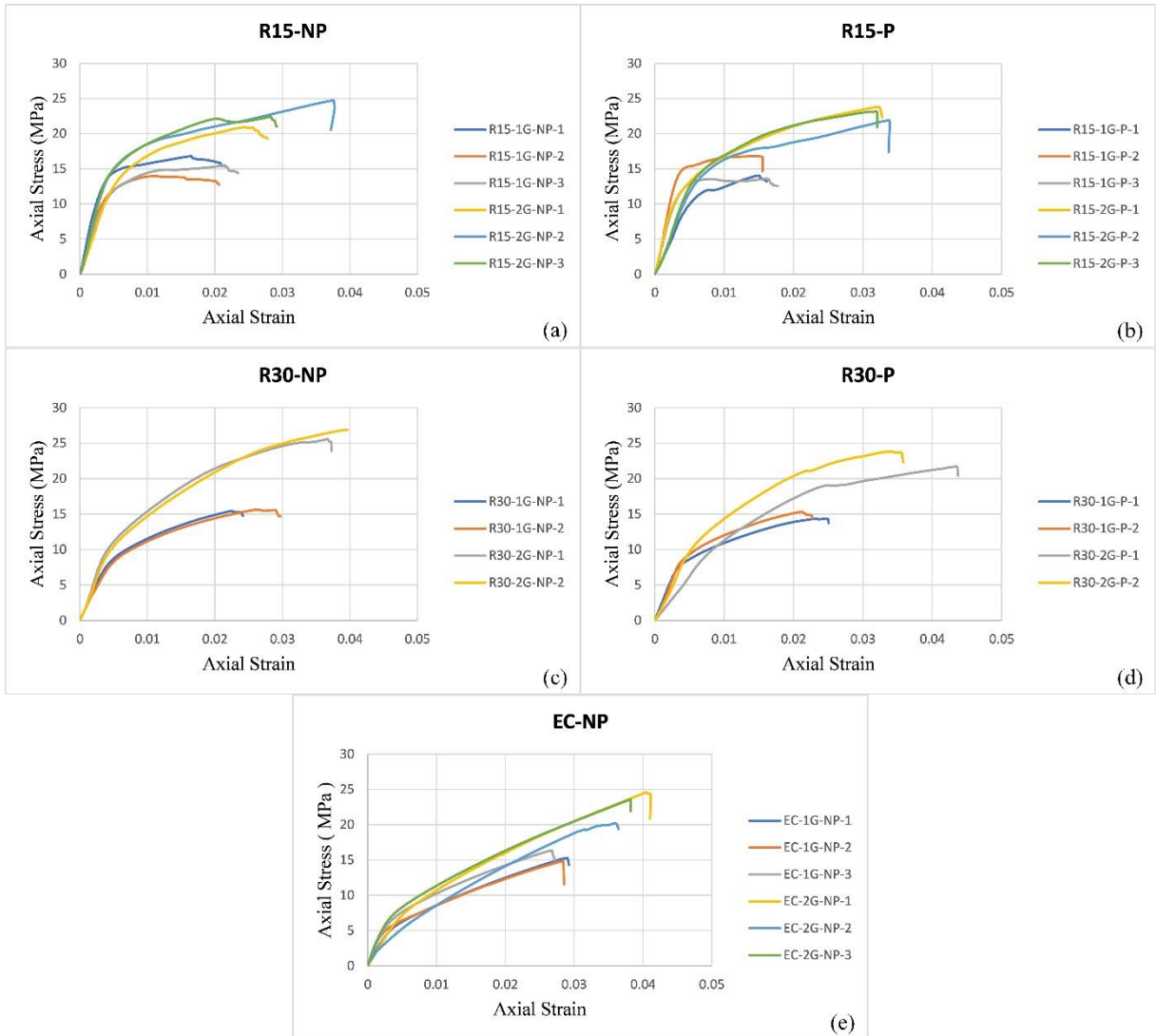
Figure 4.15. Number of GFRP layer effect
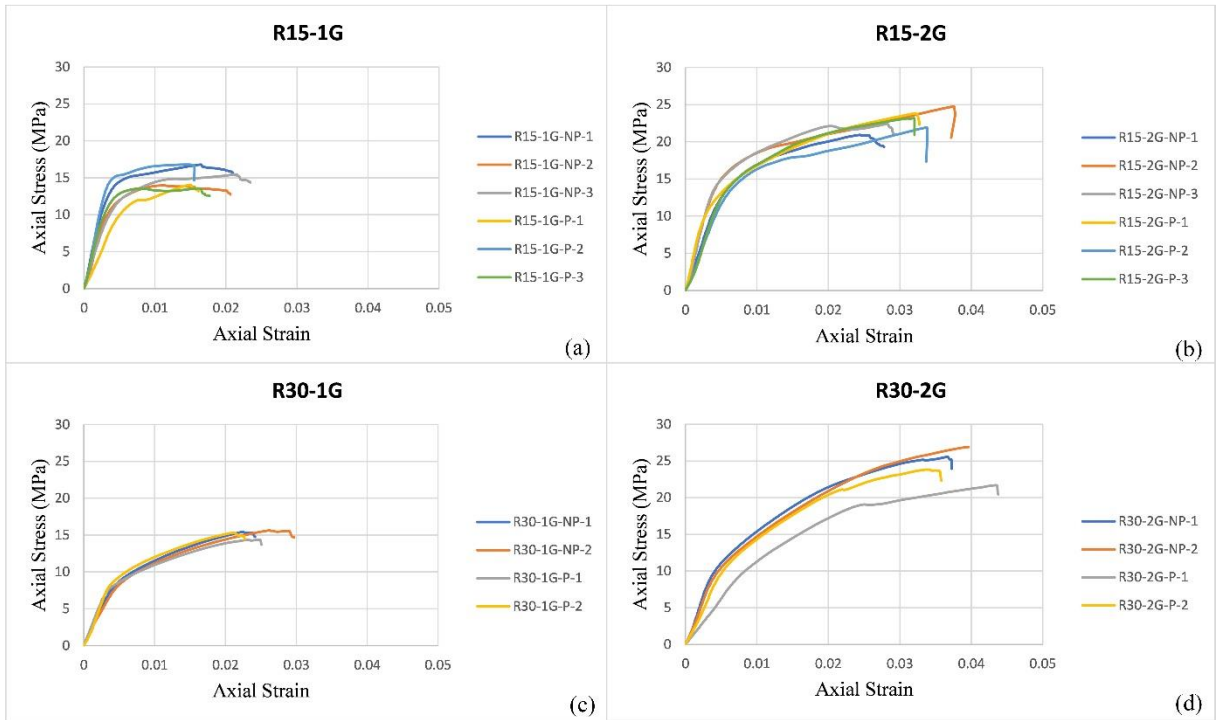
Figure 4.16. Polyurea effect
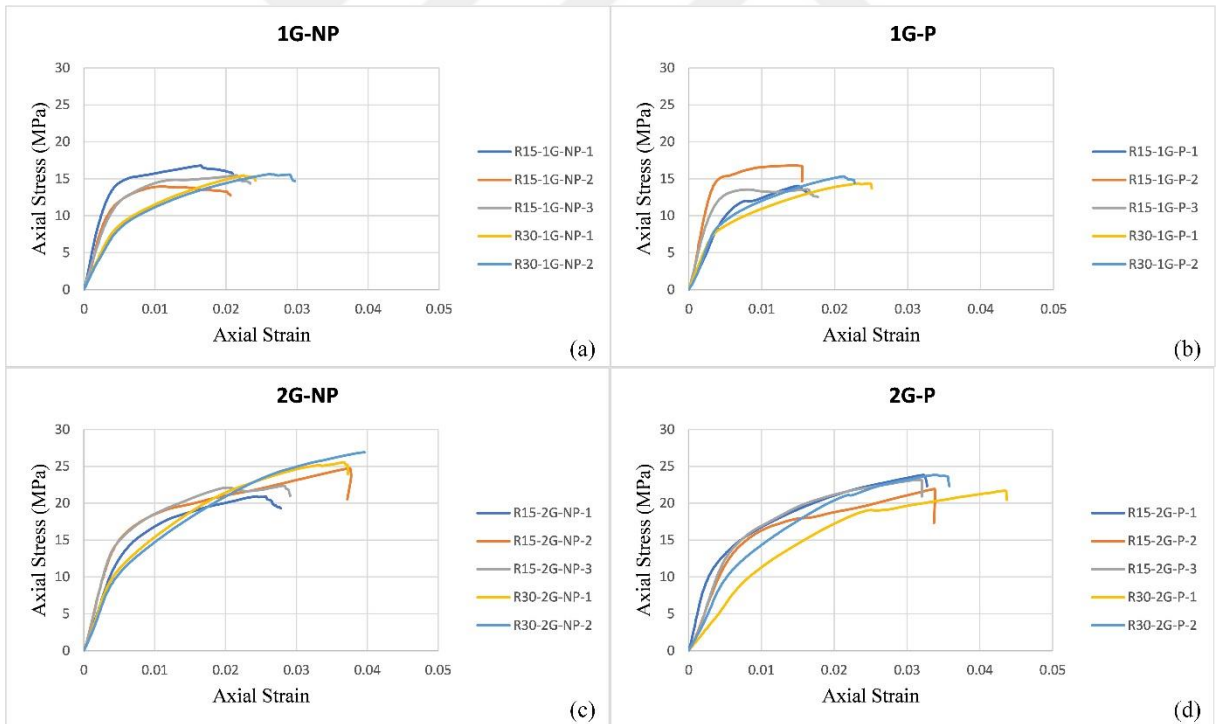
Figure 4.17. Corner radius effect
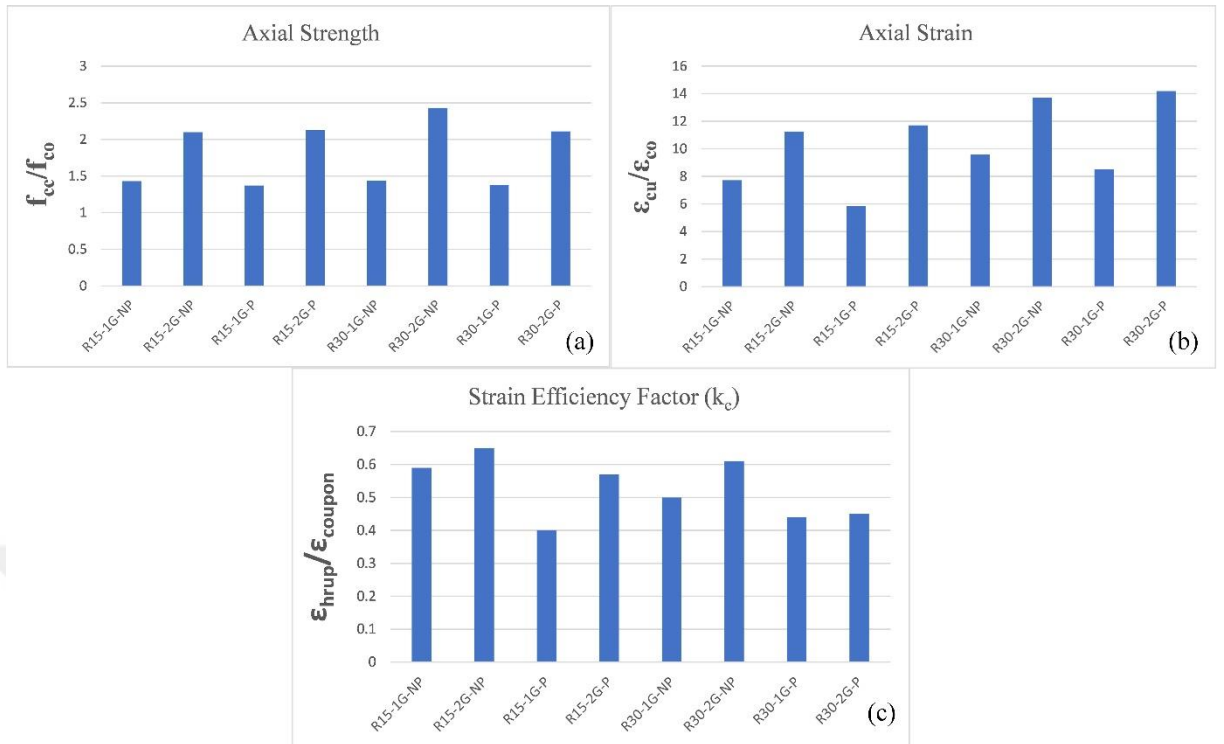
Figure 4.18. Comparisons of the strength enhancement ratios, strain enhancement ratios and strain efficiency factors of the test groups to observe the effect of the number of GFRP layers
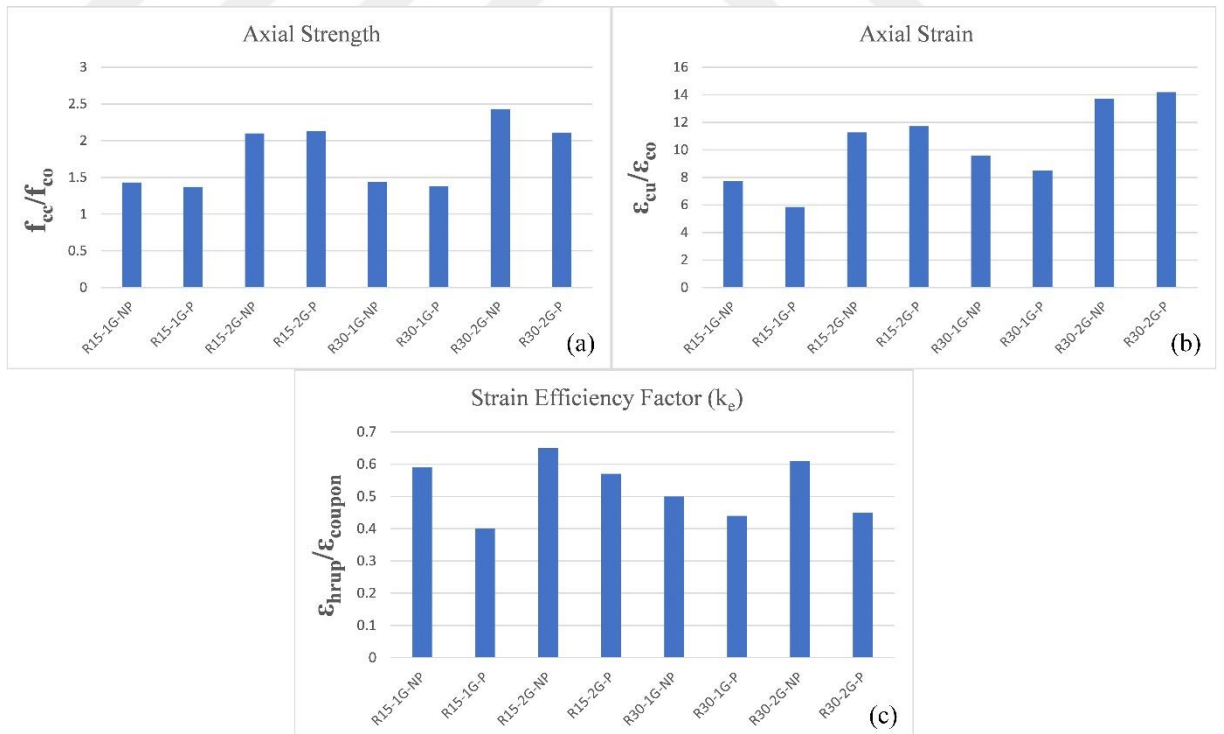
Figure 4.19. Comparisons of the strength enhancement ratios, strain enhancement ratios and strain efficiency factors of the test groups to observe the effect of the polyurea
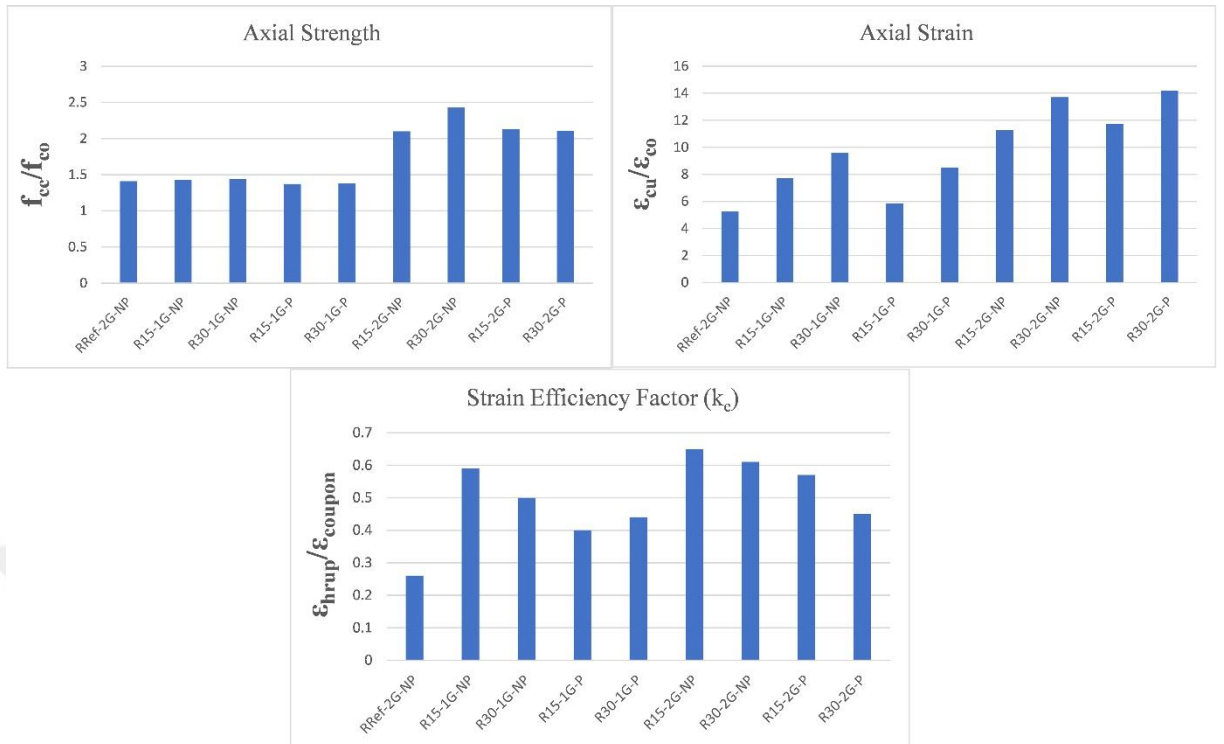
Figure 4.20. Comparisons of the strength enhancement ratios, strain enhancement ratios and strain efficiency factors of the test groups to observe the effect of the corner radius

The hoop strain vs. time graphs of the specimens are presented in Figures 4.18-22 for all test groups. Any positive contribution of polyurea was expected to be observed in these graphs. The polyurea was supposed to reduce the scattering of the hoop strains at different locations and provide a more uniform hoop strain distribution as it had been reported by Akın et al. (2020). Yet, the results do not provide any meaningful result on such a contribution of the polyurea layer for the specimens considered in this study. Further discussions on these figures will be held on in the following chapter.
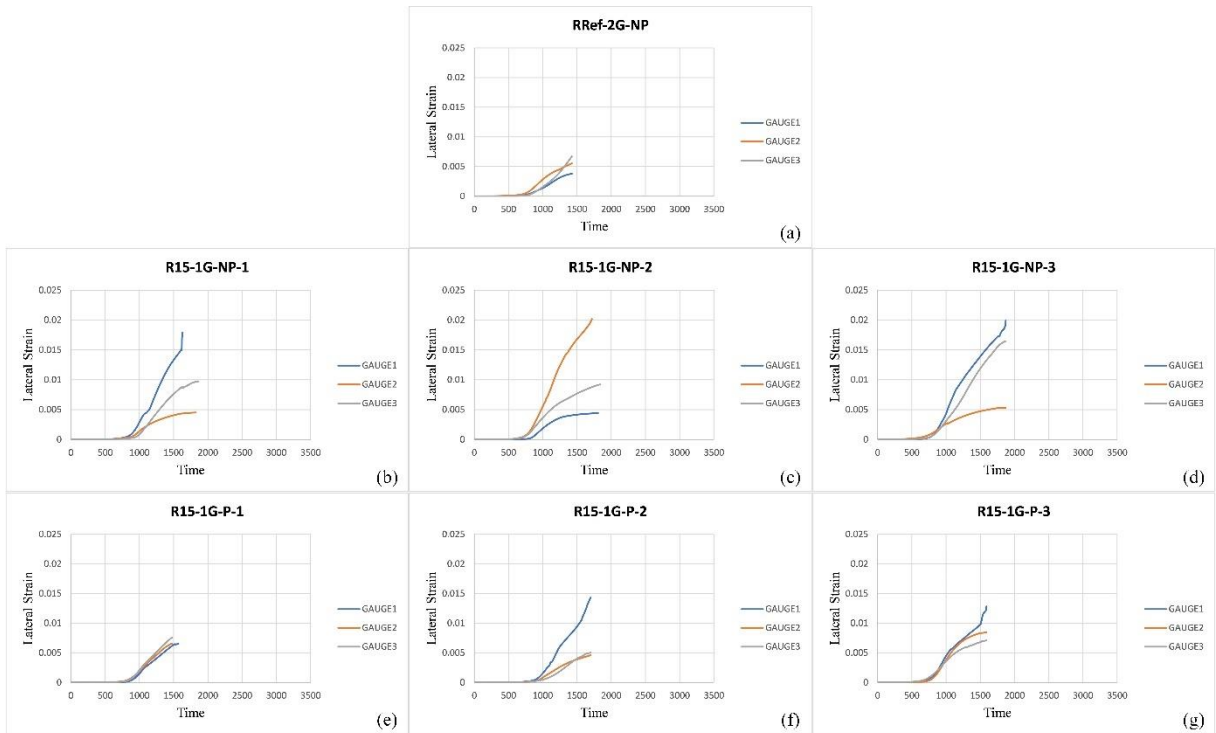
Figure 4.21. Hoop strain graphs of the RRef-2G-NP group and R15-1G groups
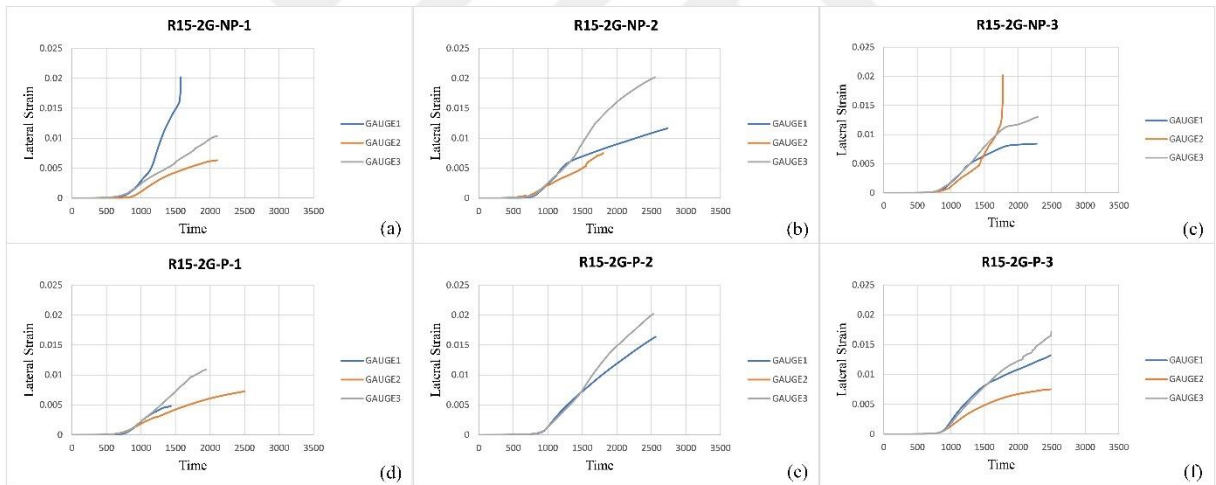
Figure 4.22. Hoop strain graphs of the R15-2G groups
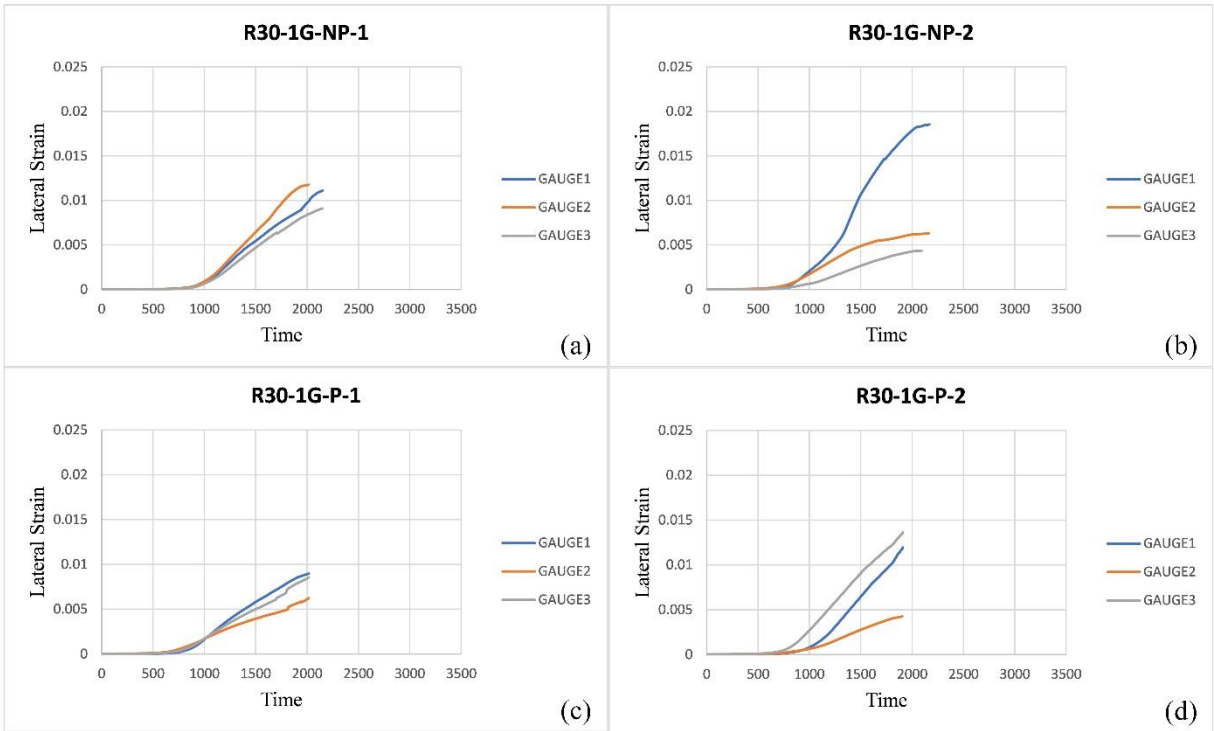
Figure 4.23. Hoop strain graphs of the R30-1G groups
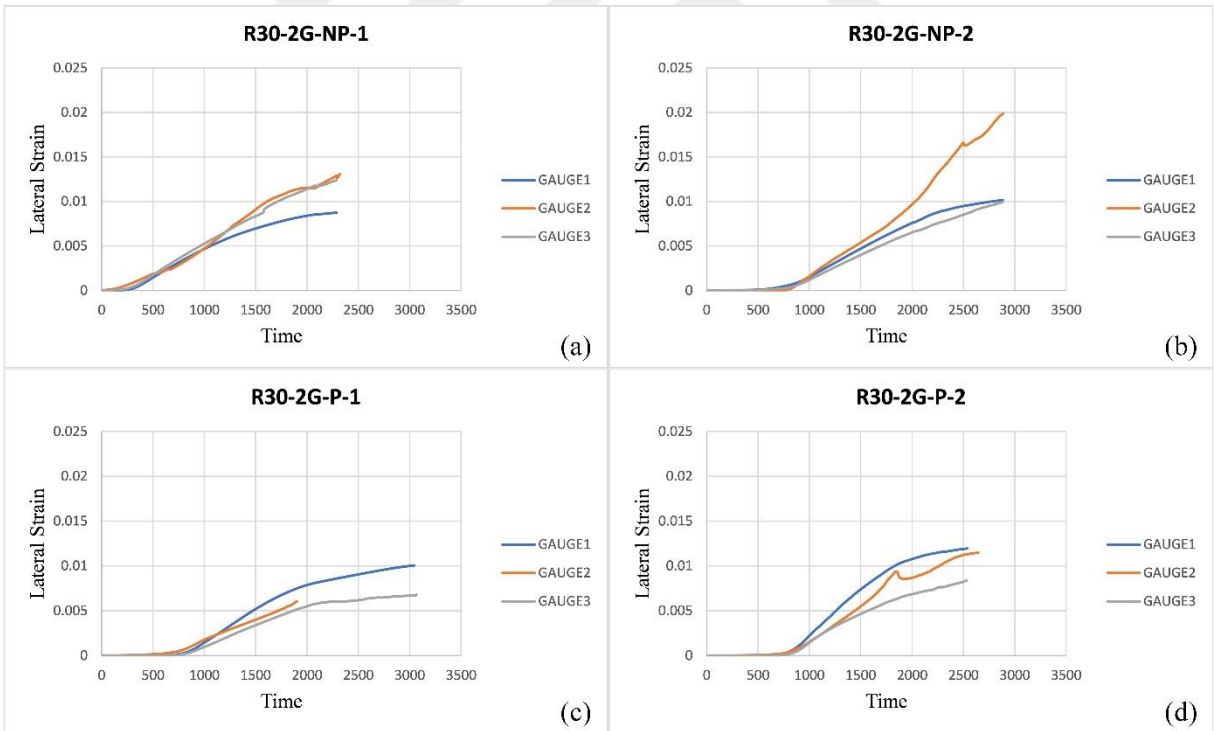
Figure 4.24. Hoop strain graphs of the R30-2G groups
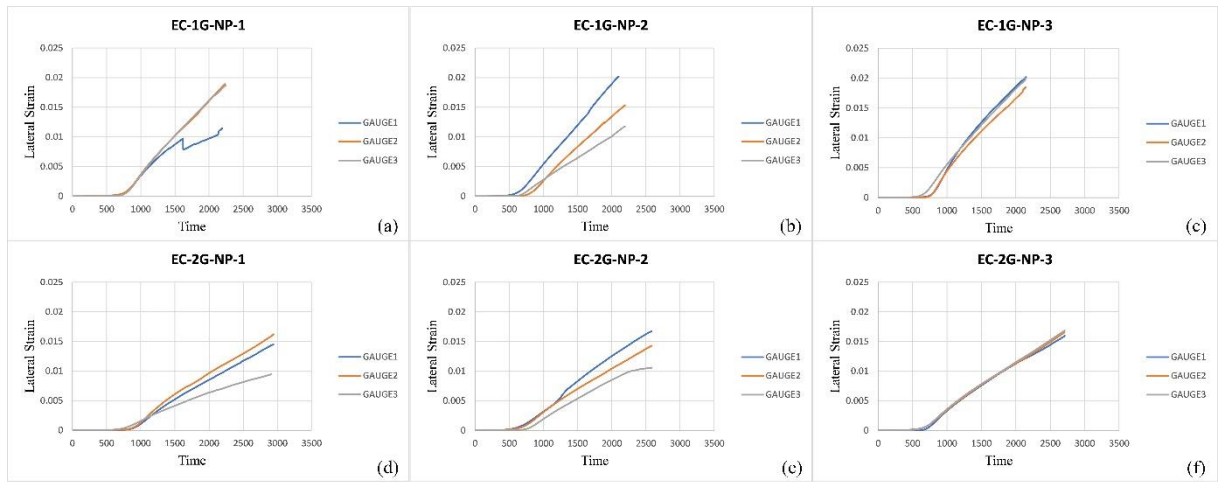
Figure 4.25. Hoop strain graphs of the EC groups

5. DISCUSSIONS

5.1. General Introduction

The main test parameters of the study were the number of GFRP layers, the corner radius, and the presence of polyurea. The effects of these three parameters were investigated in this chapter according to the previously presented test results.

5.2. Effect of the Number of FRP Layers

It is known that increasing the number of layers used in the confinement positively affects the behavior of the confined concrete. The increase in the number of GFRP layers increased the load-carrying capacity and ductility in all specimens significantly (Figure 4.15, Figure 4.18). The highest increase in the axial strength was found as 69% when the strength enhancement ratios (f_{cc}/f_{co}) of R30-1G-NP and R30-2G-NP groups were compared. The lowest increase in strength was determined to be 48% when the R15-1G-NP and R15-2G-NP groups were compared (Table 4.1). When the groups with polyurea coating were examined (R15-1G-P compared with R15-2G-P and R30-1G-P with R30-2G-P), these increments in the strength enhancement ratios were 55% and 53%, respectively (Table 4.1). Increasing the number of GFRP layers in all groups increased the strength.

When the confinement thickness was increased, the highest increase in the axial strain capacity (i.e. 100%) was observed in the R15-2G-P test group with respect to R15-1G-P. The corresponding lowest strain increase was 43% in the R30-2G-NP group with respect to R30-1G-NP. These ratios for the axial strain capacity increment were 46% and 67% in the R15-NP and R30-P test groups (i.e. 2G with respect to 1G). In general, the polyurea coated specimens seem to provide a higher increment in the axial strength when the number of confining GFRP layers was increased in comparison to those without polyurea.

The stress enhancement ratios (f_{cc}/f_{co}) for the one and two-layers of GFRP confined specimens with equivalent circular sections were 1.44 and 2.11, respectively (Table 4.1). This corresponds to a 46% increase in the axial strength due to increased confinement thickness in the circular sections. Besides, the strain capacity could be increased by 36% in the circular

sections by the increased confinement thickness. When these ratios are compared with those obtained for the rectangular sections having 15 mm or 30 mm corner radius, it may be stated that the increased confinement thickness may provoke a better enhancement in the axial response in the case of rectangular sections compared to the equivalent circular sections.

5.3. Effect of the Corner Radius

Figures 4.13-14 exhibits the effect of rounding the corners in terms of overall axial behavior of GFRP confined concrete with respect to the specimen with sharp edges. Figure 4.17 and Figure 4.20 shows the effect of increasing corner radius from 15 mm to 30 mm in different test groups. As it was previously stated, even 15 mm corner radius provided a considerable enhancement in the axial response which was further improved by rounding the corners with 30 mm radius. According to the results in Table 4.1, the specimen groups with the same parameters except corner radius were compared in terms of strength and strain-enhancement ratios (f_{cc}/f_{co} and $\varepsilon_{cu}/\varepsilon_{co}$, respectively) to assess the effect of the corner radius. The specimens with a 15 mm corner radius which are confined by two-layers of GFRP (i.e. in R15-2G-NP and R15-2G-P test groups) experienced an approximately 50% higher axial strength with respect to RRef-2G-NP. The strength-enhancement ratios (f_{cc}/f_{co}) were not altered when the corner radius was increased from 15 mm to 30 mm, except in the groups where two-layers of GFRP confinement was applied without polyurea. The axial strength was increased by about 16% in the R30-2G-NP tests group with respect to R15-2G-NP.

The strain-enhancement ratios of the R15-2G-NP and R15-2G-P test groups were 114% and 123% larger than that of specimen RRef-2G-NP. This shows that the strain-enhancement due to GFRP confinement is extremely sensitive to the rounding of corners in the rectangular sections. The strain-enhancement ratio could be increased slightly further due to the use of 30 mm corner radius with respect to 15 mm. This increment in the axial strain capacity was in the range of 21% to 24% in all groups, except those where one-layer of confinement was applied over polyurea. The strain-enhancement ratio of R30-1G-P test group was approximately 45% higher than R15-1G-P. Consequently, it may be stated that rounding of the corners (i.e. by 15 mm radius) makes a significant improvement in the confinement efficiency not only with respect to axial strength but also axial strain capacity, yet much more distinct for the latter parameter. But the axial strength improvement seems to disappear when the corner radius was

increased from 15 mm to 30 mm. And the same increase in the corner radius may only provide a slight improvement in the axial strain capacity.

.

5.4. Effect of the Polyurea

The main test parameter of this study was the presence of polyurea. Akın et al. (2020) mentioned that the hoop strain distribution became more uniform when a polyurea layer was applied before the wrapping of circular sections. It was observed that the hoop strains at different locations along the circumference attain close values at the failure state through the use of polyurea. Consequently, a higher rupture strain was reported for the polyurea applied cylindrical specimens in their study. The same observation was valid for both monotonic and cyclic axial tests. Yet, this favorable effect leads to higher ductility more explicitly only for the specimens which were subjected to cyclic axial loading. According to their results, the axial strength increment could not be observed due to the use of polyurea in any type of loading; even a slight reduction in the ultimate strength was reported.

To examine the polyurea effect, it is necessary to take a closer look at the groups with the same corner radius and the number of GFRP layers. According to Table 4.1, the value of f_{cc}/f_{co} was 2.10 in the R15-2G-NP group when polyurea was not used. When polyurea coating was used, it was 2.13 in the R15-2G-P group which was almost equal to the companion group without polyurea. When the other companion test groups with and without polyurea are compared, a slight reduction in the axial strength may be stated as it was reported by Akın et al. (2020).

According to Figures 4.21-24, no considerable favorable effect of polyurea on the hoop strain distribution along the circumference of the rectangular sections may be defined. There are signs of less scattered progression of hoop strains at different locations throughout the tests, as it was in R15-1G-P-3 (Figure 4.21.g) or R15-2G-P-2 (Figure 4.22.e) for instance. But this cannot be generalized for all the specimens having polyurea layer under the GFRP jacket. Accordingly, the average rupture strain values (and k_e ratios) could not be enhanced due to the use of polyurea in any of the test groups (Table 4.1).

According to the results of Table 4.1, the strain-enhancement ratios which may be regarded as an indicator of ductility are also compared for the companion test groups with and without polyurea. It may be stated that there was a slight improvement in the ductility of the

two-layers of GFRP confined specimens with polyurea coating where a higher confining pressure could be supplied. The same observation was valid with a 4% increased strain-enhancement ratio due to polyurea for the test groups having either 15 mm or 30 mm corner radius. On the other hand, the presence of polyurea did not make a change in the ductility for the specimens with one-layer of GFRP confinement. In these test groups (with one-layer of GFRP), the average strain-enhancement ratio decreased significantly in the polyurea applied group compared to that of companion group without polyurea.

Eventually, it may be stated that the existence of polyurea could not provide the expected favorable contribution explicitly for the low-strength concrete specimens with rectangular sections as used in this study. It should be noted that the axial loading during tests was monotonic and type of confining material was GFRP due to the limitations of the test setup. The similar specimens may exhibit a different behavior when subjected to cyclic loading, as it was the case in the study of Akın et al. (2020). Besides, the polyurea may be more beneficial in terms of enhanced ductility when different types of FRP materials which may provide a higher confinement pressure are used. This hypothesis was based on the observation on the slight ductility increase due to the use of polyurea in the specimens with two-layers of GFRP confinement with a higher confining pressure, but not in the case of one-layer of confinement with a lower confining pressure.

6. THEORETICAL INVESTIGATION

6.1. General Introduction

There are many design-oriented models that have been proposed to predict the ultimate axial strength and strain capacity of FRP confined concrete. The model of Lam and Teng (2003b) was used in this study to compare the prediction of the model with the test results of the rectangular specimens. Lam and Teng (2003b) model is an extension of the Lam and Teng (2003a) model which was proposed for the circular sections. These models are explained in the following parts.

6.2. Prediction of the Maximum Axial Stress and Strain of the Circular Columns

The model by Lam and Teng (2003a) uses Eqn. 2 to predict the maximum axial stress of the FRP confined column.

$$\frac{f_{cc}}{f_{co}} = 1 + k_1 \frac{f_{lu}}{f_{co}} \tag{2}$$

where f_{cc} is the ultimate axial strength of the confined concrete column, f_{co} is the ultimate axial strength of the unconfined concrete column, k_1 is the confinement effectiveness coefficient, and f_{lu} is the confining pressure provided by the FRP jacket. The confining pressure is provided by Eqn. 3 by assuming a uniform confinement within the section and uniform hoop strain distribution along the circumference. It should be noted that the confinement effectiveness coefficient k_1 was taken 3.3 as a constant value by Lam and Teng (2003a).

$$f_{lu} = \frac{2E_{frp}t\varepsilon_{h,rup}}{d} \tag{3}$$

where E_{frp} is the modulus elasticity of the FRP, t is the thickness of the FRP confinement, $\varepsilon_{h,rup}$ is the actual hoop rupture strain from the tests and d is the diameter of the specimen.

The ultimate axial strain of the confined concrete column can be predicted by Eqn. 4 (Lam and Teng, 2003a)

$$\frac{\varepsilon_{cu}}{\varepsilon_{co}} = 1.75 + 12 \left(\frac{f_{lu}}{f_{co}}\right)\left(\frac{\varepsilon_{h,rup}}{\varepsilon_{co}}\right)^{0.45} \tag{4}$$

where ε_{cu} is the ultimate axial strain of the confined concrete column and ε_{co} is the axial strain at the ultimate stress of the unconfined concrete column.

6.3. Prediction of the Maximum Axial Stress and Strain of the Rectangular Columns

Lam and Teng (2003b) proposed a design-oriented model for the FRP confined concrete having rectangular (and square) sections. It has been proven by the experiments that the behavior of rectangular columns is different from the circular columns (Mirmiran, 1998).
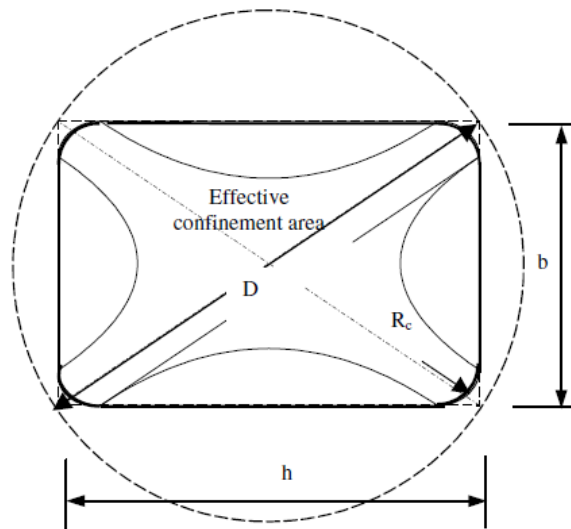
Figure 6.1. Effective confinement area in the rectangular cross-sections (Lam and Teng, 2003b)

The maximum axial strength can be calculated by Eqn. 5 according to Lam and Teng (2003b).

$$\frac{f_{cc}}{f_{co}} = 1 + k_1 k_{s1}\frac{f_{lu}}{f_{co}} \tag{5}$$

where k_1 is again considered as 3.3. The shape factor k_{s1} can be found by using Eqn. 6.

$$k_{s1} = \left(\frac{b}{h}\right)^\alpha \left(\frac{A_e}{A_c}\right) \tag{6}$$

where b and h are the column dimensions ($h \geq b$), α is a constant and taken as 2. A_e/A_c is the ratio of the effective confinement area (A_e) to the total cross-sectional area of the column (A_c) and can be found by Eqn. 7.

$$\frac{A_e}{A_c} = \frac{1 - \left((b/h)(h-2R_c)^2 + (h/b)(b-2R_c)^2/3A_g)\right) - \rho_{sc}}{1 - \rho_{sc}} \tag{7}$$

where A_g is the gross area of the column with rounded corners, p_{sc} is the ratio of the longitudinal steel reinforcement and R_c is the corner radius. A_g can be found by Eqn. 8.

$$A_g = bh - (4 - \pi)R_c^2 \tag{8}$$

The confining pressure f_{lu} can be calculated by Eqn. 9.

$$f_{lu} = \frac{2E_{frp}t\varepsilon_{h,rup}}{D} \tag{9}$$

In Eqn. 9 $\varepsilon_{h,rup}$ is defined as the rupture strain of the confining jacket obtained from the equivalent cylindrical specimens.

D is the diagonal distance of the rectangular section and can be calculated by Eqn. 10.

$$D = \sqrt{h^2 + b^2} \tag{10}$$

Lam and Teng (2003b) proposed Eqn. 11 to estimate the ultimate axial strain.

$$\frac{\varepsilon_{cu}}{\varepsilon_{co}} = 1.75 \ + \ k_2 k_{s2} \frac{f_{lu}}{f_{co}} \left(\frac{\varepsilon_{h,rup}}{\varepsilon_{co}}\right)^{0.45} \tag{11}$$

where f_{lu} is the confining pressure, k_2 was taken 12 as defined in the model. The other shape factor k_{s2} can be calculated by Eqn. 12.

$$k_{s2} = \left(\frac{h}{b}\right)^{\beta} \frac{A_e}{A_c} \tag{12}$$

where β is a constant and taken as 0.5 by the model.

6.4. Comparison of the Model Predictions with Test Results

The maximum axial stress and strain of the GFRP confined specimens were predicted by the model of Lam and Teng (2003b). Table 6.1 indicates the results of the predicted model. Calculation of f_{lu} was made in two different ways: (a) using the hoop rupture strain value of each specimen as recorded during their axial tests and (b) using the average hoop rupture strain value of the equivalent cylindrical specimens as the model suggested. The model predictions (Table 6.1) were compared with the test results (Table 4.1) and some comments were made below. These comparisons are illustrated in Figures 6.2.a and b for the strength- and strain-enhancement ratios, respectively, by a consideration of actual hoop rupture strain values of each specimen. And this is conducted by a consideration of the average hoop rupture strain of equivalent cylinders for the strength- and strain-enhancement ratios in Figures 6.3.a and b, respectively.

When we consider the actual hoop rupture strain of each specimen, the strength-enhancement ratio predictions of the Lam and Teng (2003b) model may be regarded as conservative (i.e. lower than the experimental values) (Figure 6.2.a). The test results and the model predictions in terms of f_{cc}/f_{co} are more compatible for the specimens confined with one layer of GFRP. Yet, there is an approximately 23% difference between the model predicted and

experimentally obtained f_{cc}/f_{co} values even in the one-layer of GFRP confinement. This difference becomes 46% for the two-layers of confinement which is even more conservative compared to those with one-layer of GFRP confinement. In general, the other test parameters (i.e. the presence of polyurea and corner radius) seems to have only negligible effect on these statements.

When we consider the actual rupture strain of each specimen, the model predictions were again generally lower than the test results for the case of strain enhancement ratios ($\varepsilon_{cu}/\varepsilon_{co}$) (Table 6.1 and Figure 6.2.b). The difference between the model predicted and experimentally obtained $\varepsilon_{cu}/\varepsilon_{co}$ ratios change between 15% and 46%. The difference was slightly less for the 15 mm corner radius compared to 30 mm. Besides, the model prediction may be regarded as more successful for the two-layers of GFRP confinement without polyurea.

When we use the average hoop rupture strain of the equivalent cylindrical specimens for the model predictions of f_{cc}/f_{co}, the predicted values become only slightlty closer to the test results compared to the case when actual hoop rupture strain of each specimen was considered (Table 6.1 and Figure 6.3.a). The same statements for the one- and two-layers of GFRP confinement which was mentioned in the case of considering the actual rupture strain of the specimens are again valid here. In general, it may be concluded that the unsatisfactory and conservative f_{cc}/f_{co} predictions of the Lam and Teng (2003b) does not change significantly for the use of hoop rupture strain values obtained from the tests of each specimen or from the equivalent cylindrical specimens.

When we use the average hoop rupture strain of the equivalent cylindrical specimens for the model predictions of $\varepsilon_{cu}/\varepsilon_{co}$, the predicted and experimentally obtained values become more compatible (Figure 6.3.b). As different than the previous cases, the model predictions may become to be unconservative in some of the specimens. This was more obvious for all the specimens of R15-1G-P test group, where the highest difference between the predicted and experimentally obtained $\varepsilon_{cu}/\varepsilon_{co}$ ratios occurred with 27%. In the other test groups, this difference remain between 3% and 9%.

In general, the unsatisfactory performance of the Lam and Teng model (2003b) for the f_{cc}/f_{co} ratio may be attributed to the considerably small shape factor for the strength-enhancement (k_{s1}) that is calculated for the rectangular sections having a cross-sectional aspect ratio of "1:2" as it is for the specimens of this study (67 mm:134 mm). In a simultaneous thesis study which was conducted with the same parameters as in this study but for the square sections

(i.e. aspect ratio of "1:1"), no such incompatibility was observed. Besides, it should be noted that the Lam and Teng (2003a) model which was taken as a basis for Lam and Teng (2003b) has proven to be quite accurate in many different studies for various cases (i.e. different unconfined concrete strength, type of FRP, etc.) (Ozbakkaloglu and Akin, 2012; Akın et al., 2020). The only change for the Lam and Teng (2003b) model is the shape factor, k_{s1} in the f_{cc}/f_{co} expression of Lam and Teng (2003a) model. The k_{s1} factor was equal to 0.25 for the specimens of this study. Due to the use of such a small value for the shape factor, the second component (i.e. $k_1.k_{s1}.f_{lu}/f_{co}$) in the f_{cc}/f_{co} expression becomes to be a small number and tend to be insensitive to the change in the confining pressure (f_{lu}).

Table 6.1. Predictions of the Model (Lam and Teng 2003b)

TEST GROUP	SPECIMEN	Experimental Results				Model Predictions					
		Avg. f_{cc}/f_{co}	Avg. $\varepsilon_{cu}/\varepsilon_{co}$	ε_{hrup} [1]	ε_{hrup} [2]	f_{cc}/f_{co} [1]	Avg. f_{cc}/f_{co} [1]	$\varepsilon_{cu}/\varepsilon_{co}$ [1]	Avg. $\varepsilon_{cu}/\varepsilon_{co}$ [1]	f_{cc}/f_{co} [2]	$\varepsilon_{cu}/\varepsilon_{co}$ [2]
R15-1G-NP	**1**	1.43	7.72	0.0107	0.0172	1.076	1.085	4.62	5.12	1.12	7.44
	2			0.0112		1.080		4.83			
	3			0.0139		1.099		5.93			
R15-1G-P	**1**	1.37	5.85	0.0068	0.0172	1.049	1.057	3.26	3.68	1.12	7.44
	2			0.0080		1.057		3.64			
	3			0.0094		1.067		4.14			
R15-2G-NP	**1**	2.10	11.26	0.0122	0.0145	1.175	1.186	8.74	9.41	1.21	10.69
	2			0.0131		1.186		9.42			
	3			0.0138		1.197		10.08			
R15-2G-P	**1**	2.13	11.72	0.0076	0.0145	1.109	1.162	5.27	8.15	1.21	10.69
	2			0.0139		1.198		10.15			
	3			0.0126		1.179		9.02			
R30-1G-NP	**1**	1.44	9.58	0.0106	0.0172	1.097	1.092	5.39	5.16	1.16	9.04
	2			0.0097		1.088		4.94			
R30-1G-P	**1**	1.38	8.51	0.0079	0.0172	1.072	1.081	4.11	4.57	1.16	9.04
	2			0.0099		1.090		5.04			
R30-2G-NP	**1**	2.43	13.71	0.0114	0.0145	1.207	1.224	9.77	10.79	1.26	13.20
	2			0.0133		1.242		11.81			
R30-2G-P	**1**	2.11	14.19	0.0076	0.0145	1.139	1.166	6.24	7.60	1.26	13.20
	2			0.0105		1.193		8.96			

(1) The model predictions where the rupture strain of the specimens with rectangular section is considered

(2) The model predictions where the rupture strain of the specimens with equivalent circular section is considered

Figure 6.2. Comparison of model predictions of (a) strength-enhancement and (b) strain-enhancement ratios with experimental results by considering rupture strain of each specimen
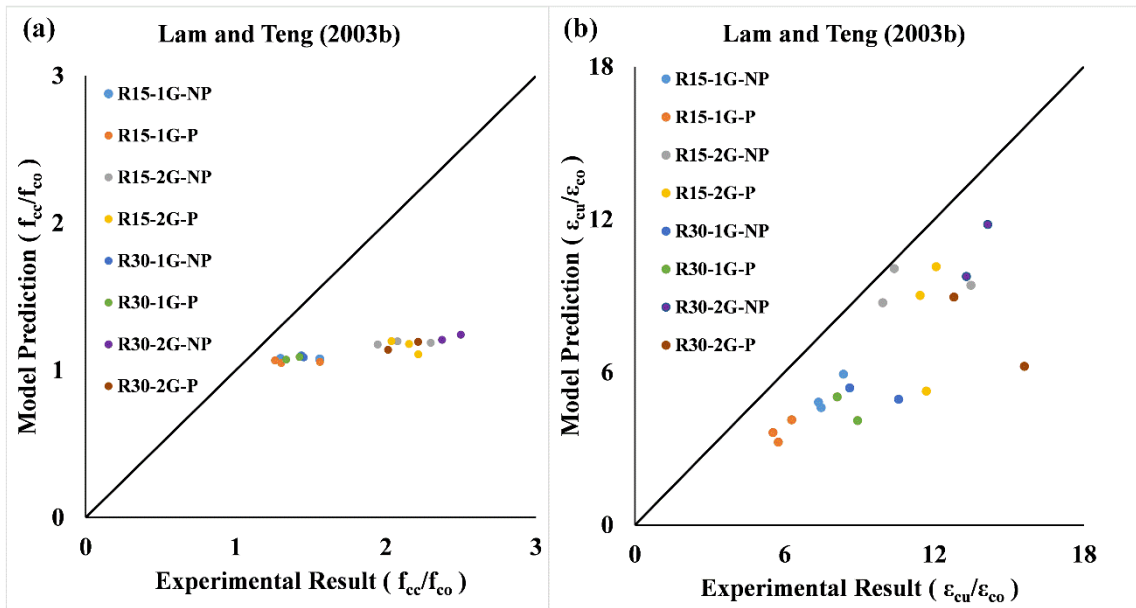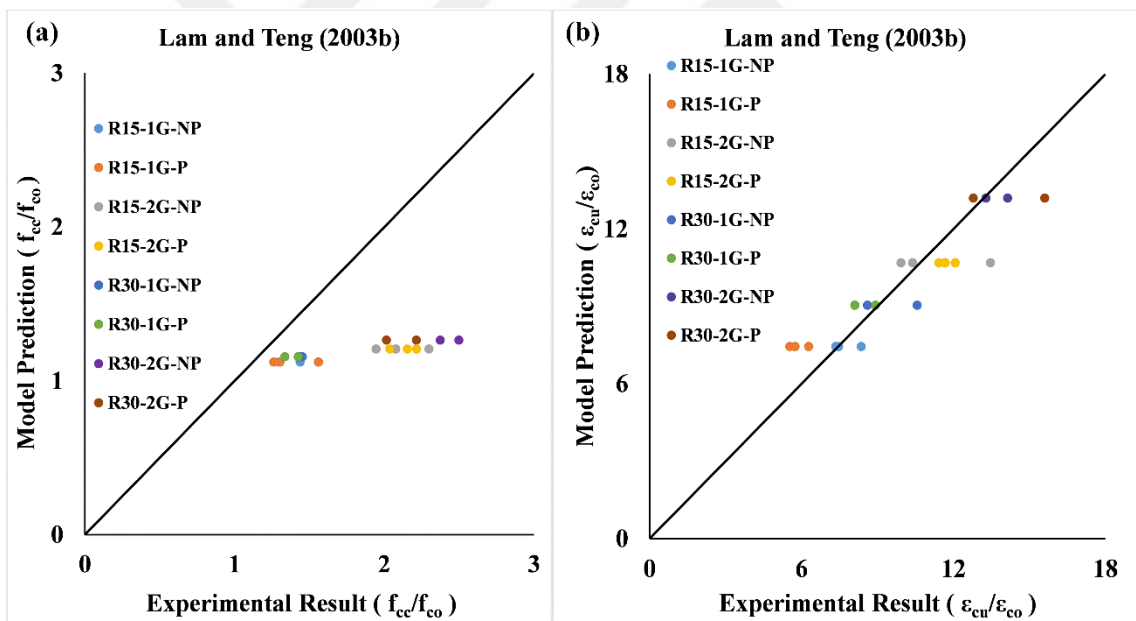

Figure 6.3. Comparison of model predictions of (a) strength-enhancement and (b) strain-enhancement ratios with experimental results by considering rupture strain of equivalent cylindrical specimen

63

7. CONCLUSIONS

7.1. General Introduction

The main test parameters of the study are the number of GFRP layers, the corner radius and the presence of polyurea. The behavior of rectangular concrete columns with these parameters was evaluated under the monotonic axial compressive loading. Consequently, the following conclusions can be made. These conclusions should not be generalized without due judgement or unless supported by further experimental results.

1. When the rectangular specimens with low strength concrete were subjected to monotonic loading, increasing the confinement thickness significantly increased the axial strength and strain capacity in all groups. The highest strength increment was observed as 69 % in the specimens that have a 30 mm corner radius without polyurea coating when the two-layers of GFRP used in confinement instead of one-layer. The axial strain enhancement seems to be better improved by the increased confinement thickness in the polyurea coated specimens.

2. When the axial strength values enhanced by increasing the confining layers from one to two was assessed for the rectangular and equivalent circular sections, it may be stated that the rectangular sections may be more sensitive to the increased confinement thickness according to the results of this study.

3. The rounding of the sharp edges (i.e. specimens with 15 mm corner radius with respect to RRef-2G-NP) makes a considerable difference in terms of not only strength- but also strain-enhancement ratios. However, this was more significant for the axial strain capacity. On the other hand, the improvement in the axial response due to increasing the corner radius from 15 mm to 30 mm remained to be more limited. There was no alteration in the strength-enhancement ratio and only a slight improvement could be provided in terms of strain-enhancement ratio.

4. The presence of a polyurea layer that was provided between the core concrete and the confining GFRP jacket could not lead to the anticipated improvement in the rupture strain levels. The axial strength-enhancement remained slightly lower in the case of test groups with polyurea when compared with the similar test group without

polyurea. This result was similar to the observation of Akın et al. (2020). The axial strain-enhancement ratio could be slightly improved when the polyurea layer was present under two-layers of GFRP confinement. Yet, no such improvement was observed for the one-layer of GFRP confinement. It is believed that the low tensile strength of the GFRP material inhibits the anticipated utilization of the polyurea by protecting the jacket from the stress concentrations caused by the damaging of the concrete. The GFRP jacket ruptures without forming a significant confinement pressure on the concrete core and the less damage occurs in the concrete core at the failure state. When the damage in the concrete core is low, the stress concentrations does not take place considerably. As it was also reported by Akın et al. (2020), the effect of polyurea may be more obvious in the case of cyclic test results. Besides, the use of different types of FRP materials which may provide higher confining pressure may also be taken into consideration to observe any favorable effect of polyurea in the axial response.

5. Lam and Teng (2003b) model could not predict the strength-enhancement ratio close to the test results. The predictions were considerably conservative with respect to the values obtained from the tests which was not changed by using different hoop rupture strain values (i.e. either actual rupture strain for each specimen or rupture strain from the equivalent cylindrical specimens). The extremely small shape factor, k_{s1} that is calculated for the rectangular section with a cross-sectional aspect ratio of 1:2 may be the reason of the unsatisfactory predictions of f_{cc}/f_{co}. Therefore, a better definition of this shape factor considering different cross-sectional aspect ratios may be required.

6. The strain-enhancement ratio predictions of the Lam and Teng (2003b) model was again conservative with respect to the test results when the actual rupture strain values were utilized in the model. Whereas, the predicted $\varepsilon_{cu}/\varepsilon_{co}$ ratios become more close to the test results when the average hoop rupture strain of the equivalent cylindrical specimens were used as suggested by the Lam and Teng (2003b) model.

REFERENCES

Akın, E., Tunaboyu, O., Avşar, Ö. (2020). Axial behavior of FRP confined low-strength concrete with polyurea. *Structures*, *28*(October), 1774–1784. https://doi.org/10.1016/j.istruc.2020.10.015

ASTM C39 / C39M – 20 (2020). Standard test method for compressive strength of cylindrical concrete specimens. ASTM International, West Conshohocken, PA.

ASTM D3039 / D3039M – 17 (2017). Standard test method for tensile properties of polymer matrix. ASTM International, West Conshohocken, PA.

Avci, H., Hassanin, A., Hamouda, T., Kılıç, A. (2019). High performance fibers: a review on current state of art and future challenges. *Eskişehir Osmangazi Üniversitesi Mühendislik ve Mimarlık Fakültesi Dergisi*, *27*(2), 130–155. https://doi.org/10.31796/ogummf.537704

Benzaid, R., Chikh, N.E., Mesbah, H. (2008). Behaviour of square concrete column confined with GFRP composite WARP. *Journal of Civil Engineering and Management*, *14*(2), 115–120. https://doi.org/10.3846/1392-3730.2008.14.6

Choi, E., Choi, D.H., Chung, Y. S., DesRoches, R. (2012). Seismic protection of lap-spliced RC columns using SMA wire jackets. *Magazine of Concrete Research*, *64*(3), 239–252. https://doi.org/10.1680/macr.10.00181

Green, M.F., Bisby, L.A., Fam, A. Z., Kodur, V.K.R. (2006). FRP confined concrete columns: behaviour under extreme conditions. *Cement and Concrete Composites*, *28*(10), 928–937. https://doi.org/10.1016/j.cemconcomp.2006.07.008

Kalyoncuoglu, A., Ghaffari, P., Goksu, C., Ilki, A. (2013). Rehabilitation of corrosion-damaged substandard RC columns using FRP sheets. *Advanced Materials Research*, *639–640*(1), 1096–1103. https://doi.org/10.4028/www.scientific.net/AMR.639-640.1096

Karbhari, V.M. and Lee, L.S. (2010). Service life estimation and extension of civil engineering structures. In *Service Life Estimation and Extension of Civil Engineering Structures*. https://doi.org/10.1533/9780857090928

Lam, L. and Teng, J.G. (2003a.) Design-oriented stress–strain model for FRP-confined concrete. *Construction and Building Materials*, 17, 471-489. doi:10.1016/S0950-0618(03)00045-X

Lam, L. and Teng, J.G. (2003b). Design-oriented stress–strain model for FRP-confined concrete in rectangular columns. *Reinforced Plastics and Composites*, 22, 1149–38. doi:10.1177/073168403035429

Lam, L. and Teng, J.G. (2009). Stress-strain model for FRP-confined concrete under cyclic axial compression. *Engineering Structures*, *31*(2), 308–321. https://doi.org/10.1016/j.engstruct.2008.08.014

Mirmiran, A., Shahawy, M., Samaan, M., Echary, H. El, Mastrapa, J.C., Pico, O. (1998). Effect of column parameters on FRP-confined concrete. *Journal of Composites for Construction*, *2*(4), 175–185. https://doi.org/10.1061/(asce)1090-0268(1998)2:4(175)

Ozbakkaloglu, T. and Akın, E. (2012). Behavior of FRP-confined normal- and high-strength concrete under cyclic axial compression. Journal of Composites for Structures, vol. 16, no. 4, pp. 451–463. doi:10.1061/(ASCE) CC.1943-5614.0000273

Parniani, S. and Toutanji, H. (2015). Monotonic and fatigue performance of RC beams strengthened with a polyurea coating system. *Construction and Building Materials*, *101*, 22–29. https://doi.org/10.1016/j.conbuildmat.2015.10.020

Pham, T.M., Youssed, J., Hadi, M.N.S., Tran, T.M. (2016). Effect of different FRP wrapping arrangements on the confinement mechanism. *Procedia Engineering*, *142*, 307–313. https://doi.org/10.1016/j.proeng.2016.02.051

Pudjisuryadi, P., Tavio, T., Suprobo, P. (2015). Performance of square reinforced concrete columns externally confined by steel angle collars under combined axial and lateral load. *Procedia Engineering*, *125*, 1043–1049. https://doi.org/10.1016/j.proeng.2015.11.160

Raval, R. and Dave, U. (2013). Behavior of GFRP wrapped RC columns of different shapes. *Procedia Engineering*, *51*(NUiCONE 2012), 240–249. https://doi.org/10.1016/j.proeng.2013.01.033

Raza, S., Khan, M.K.I., Menegon, S.J., Tsang, H.H., Wilson, J.L. (2019). Strengthening and repair of reinforced concrete columns by jacketing: state-of-the-art review. *Sustainability (Switzerland)*, *11*(11). https://doi.org/10.3390/su11113208

Rousakis, T.C. and Tepfers, R. (2001). Experimental investigation of concrete cylinders

confined by carbon FRP sheets under monotonic and cyclic compressive load. Research Report. Göteborg, Sweden: Chalmers University of Technology.

Safan, M. (2004). Strength of short square columns confined with GFRP wraps. *Engineering Research Journal*, *27*(1), 83–90. https://doi.org/10.21608/erjm.2004.82614

Sonnenschein, R., Gajdosova, K., Holly, I. (2016). FRP composites and their using in the construction of bridges. *Procedia Engineering*, *161*, 477–482. https://doi.org/10.1016/j.proeng.2016.08.665

Stepanek, P., Girgle, F., Kostiha, V., Matusikova, A. (2016, October 26-29). *Experimental study of concrete columns strengthening by FRP fabric confinement*. Twelfth International Conference on Structural Repair and Rehabilitation, Porto, Portugal.

Tankut, T. (2005, September 22-24). *Türkiye'deki bina yapıları için güçlendirme stratejisi*. Antalya Yöresinin İnşaat Mühendisliği Sorunları Kongresi, Bildiriler kitabı, Antalya, Turkey.

Vandoros, K. G. and Dritsos, S.E. (2008). Concrete jacket construction detail effectiveness when strengthening RC columns. *Construction and Building Materials*, *22*(3), 264–276. https://doi.org/10.1016/j.conbuildmat.2006.08.019

T.C

AYDIN ADNAN MENDERES UNIVERSITY
GRADUATE SCHOOL OF NATURAL AND APPLIED SCIENCES

SCIENTIFIC ETHICAL STATEMENT

I hereby declare that I composed all the information in my master's thesis entitled AXIAL BEHAVIOUR OF FRP CONFİNED RECTANGULAR COLUMNS WITH POLYUREA within the framework of ethical behaviour and academic rules, and that due references were provided and for all kinds of statements and information that do not belong to me in this study in accordance with the guide for writing the thesis. I declare that I accept all kinds of legal consequences when the opposite of what I have stated is revealed.

CURRICULUM VITAE

Last name, First name: KARAYİĞEN, Sinan

Nationality: Turkish

Foreign language: English

Education: B.Sc. of Civil Engineering – Adnan Menderes University, Aydın.

Level	Institute	Date of graduation
Bachelor's	Faculty of Engineering	10/06/2019